Aus dem Institut für Molekularbiologie

(Prof. Dr. rer. nat. M. T. Bohnsack)

Im Zentrum Biochemie und Molekulare Zellbiologie

der Medizinischen Fakultät der Universität Göttingen

Characterisation of the RNA modifying enzyme ABH1

INAUGURAL-DISSERTATION

zur Erlangung des Doktorgrades

der Medizinischen Fakultät der

Georg-August-Universität zu Göttingen

vorgelegt von

Benedikt Hübner

aus

München

Göttingen 2021

Dekan:	Prof. Dr. med. W. Brück
Referent:	Prof. Dr. rer. nat. M. T. Bohnsack
Ko-Referent:	Prof. Dr. rer. nat. M. Meinecke
Drittreferent:	Prof. Dr. med. R. Dressel

Datum der mündlichen Prüfung: 03.05.2022

Die Daten, auf denen die vorliegende Arbeit basiert, wurden teilweise publiziert:

Haag S, Sloan KE, Ranjan N, Warda AS, Kretschmer J, Blessing C, **Hübner B**, Seikowski J, Dennerlein S, Rehling P et al. (2016): NSUN3 and ABH1 modify the wobble position of mt-tRNA^{Met} to expand codon recognition in mitochondrial translation. EMBO J 35, 2104-2119

Table of Contents

List of Figures ..... **III**
List of Tables ..... **IV**
Abbreviations ..... **VI**
1 Introduction **1**
1.1 RNA modifications 1
1.1.1 General overview 1
1.1.2 mRNA, rRNA and tRNA modifications and their functions 1
1.1.3 Dynamics of RNA modifications 5
1.1.4 RNA modifications and disease 7
1.2 5-Methylcytosine and its derivatives in RNA 10
1.2.1 m^5C and m^5C RNA methyltransferases 10
1.2.2 5-Formylcytosine in tRNA 11
1.3 Cellular roles of mitochondria 11
1.3.1 Mitochondrial translation 12
1.3.2 Mitochondrial RNA modifications 13
1.3.3 Mitochondrial RNA modifications and disease 15
1.4 Aim of the thesis 17
2 Materials and Methods **18**
2.1 Materials 18
2.1.1 Devices, consumables and chemicals 18
2.1.2 Buffers and solutions 24
2.1.3 Cell lines and cell culture media 31
2.1.4 RNAs, oligonucleotides, vectors and recombinant proteins 32
2.1.5 Software 34
2.2 Methods 35
2.2.1 Cell culture 35
2.2.2 RNA interference 35
2.2.3 Total RNA extraction 36
2.2.4 Complementary DNA synthesis 36
2.2.5 Quantitative polymerase chain reaction 36
2.2.6 Cross-linked RNA immunoprecipitation 37
2.2.7 RNA bisulfite sequencing 39
2.2.8 Molecular cloning 41
2.2.9 Site-directed mutagenesis 44

2.2.10 Protein expression 46
2.2.11 Protein purification 46
2.2.12 Determining protein concentration 47
2.2.13 Sodium dodecyl sulfate-polyacrylamide gel electrophoresis analysis 47
2.2.14 *in vitro* transcription 48
2.2.15 *in vitro* methylation-oxidation assay 48
3 Results 52
3.1 Background 52
3.2 Interaction of ABH1 and mt-tRNA^{Met} 52
3.3 *in vitro* oxidation of m^{5}C34 of mt-tRNA^{Met} by ABH1 53
3.3.1 ABH1 can be efficiently depleted by RNA interference 59
3.4 Analysis of the role of ABH1 in forming f^{5}C34 in mt-tRNA^{Met} *in vivo* 60
4 Discussion 63
4.1 Modification pathway of C34 of mt-tRNA^{Met} 63
4.1.1 Methylation by NSUN3 63
4.1.2 ABH1 in the production of f^{5}C34 of mt-tRNA^{Met} 64
4.1.3 Relative amounts of m^{5}C and f^{5}C detected at position 34 of mt-tRNA^{Met} 65
4.1.4 Function of f^{5}C in expanding codon recognition by mt-tRNA^{Met} 66
4.2 Target spectrum of ABH1 67
4.3 Role of RNA modifications in co-ordinating cells response to metabolic status 68
4.4 Mitochondrial tRNA modifications and disease 69
4.4.1 Pathogenic mutations in *NSUN3* 69
4.4.2 Pathogenic mutations identified in mt-tRNA^{Met} 69
5 Summary 71
6 References 73

List of Figures

Figure 1: tRNA modifications in *Saccharomyces cerevisiae*. 4
Figure 2: Dynamics of the RNA modification m^6A in mRNA. 6
Figure 3: RNA modifications and their links to human disease. 8
Figure 4: Maps of vectors used for molecular cloning. 41
Figure 5: mt-$tRNA^{Met}$ is specifically associated with NSUN3 and ABH1. 53
Figure 6: Cloning of ABH1 for recombinant protein expression. 54
Figure 7: Coding sequence of ABH1 with mutation sites and sequencing results. 55
Figure 8: Expression and purification of recombinant ABH1 and mutants from *Escherichia coli*. 56
Figure 9: Reaction scheme of methylation and oxidation of C34 in mt-$tRNA^{Met}$. 57
Figure 10: Oxidation of m^5C34 of mt-$tRNA^{Met}$ by ABH1 *in vitro*. 58
Figure 11: Depletion of ABH1 by RNA interference. 60
Figure 12: Reaction scheme of reduced and non-reduced bisulfite treatment of cytosines. 61
Figure 13: Deep sequencing data after reduced and non-reduced bisulfite treatment. 62

List of Tables

Table 1: Devices and equipment 18
Table 2: Consumables 19
Table 3: Chemicals and kits 20
Table 4: BPTE buffer (10 x) 24
Table 5: Coomassie staining solution 25
Table 6: Colloidal coomassie staining solution 25
Table 7: Dialysis buffer I 25
Table 8: Dialysis buffer II 25
Table 9: Fixing solution 25
Table 10: High stringency buffer 26
Table 11: IMAC elution buffer 26
Table 12: IMAC washing buffer 26
Table 13: Laemmli buffer 26
Table 14: Methylation buffer (10 x) 27
Table 15: $NaBH_4$ solution 27
Table 16: Ni-NTA washing buffer I 27
Table 17: Ni-NTA washing buffer II 27
Table 18: Ni-NTA washing buffer III 28
Table 19: Oxidation buffer 28
Table 20: PBS buffer (10 x) 28
Table 21: Phosphate buffer (10 mM) 28
Table 22: Pre-hybridisation buffer 29
Table 23: PreScission eluate buffer 29
Table 24: RNA loading dye 29
Table 25: Sonication buffer 29
Table 26: SSC buffer (20 x) 29
Table 27: TAE buffer (50 x) 30
Table 28: TBE buffer (10 x) 30
Table 29: TMN 150 buffer 30
Table 30: TMN 1000 buffer 30
Table 31: Eukaryotic cell lines 31
Table 32: Lysogeny broth media solution 31
Table 33: Lysogeny broth agar 31
Table 34: Lysogeny broth amp-agar 31
Table 35: Lysogeny broth amp-can media 31

Table 36: Lysogeny broth kan-agar 32
Table 37: HEK 293 cell lines for expression of HisPrcFLAG- tagged dioxygenases 32
Table 38: RNAs 32
Table 39: Oligonucleotides 32
Table 40: Vectors and templates 33
Table 41: His-MBP-tagged recombinant proteins 34
Table 42: Software 34
Table 43: Reaction assay of qPCR with complementary DNA 37
Table 44: qPCR programme 37
Table 45: PAA gel mix 39
Table 46: Reaction assay of PCR for amplification of ABH1 coding sequence 42
Table 47: Programme of PCR for amplification of ABH1 coding sequence 42
Table 48: Restriction digest of purified ABH1 amplicon or target vectors 43
Table 49: Ligation reaction of ABH1 insert and target vectors 43
Table 50: Reaction assay of PCR for amplification of ABH1 mutants 45
Table 51: Programme of PCR for amplification of ABH1 mutants 45
Table 52: Components for SDS-PAGE (sufficient for two 12 % gels) 47
Table 53: *in vitro* transcription 48
Table 54: Methylation assay 49
Table 55: Oxidation assay 50
Table 56: Components of 12 % denatured urea PAGE 51

Abbreviations

(q)PCR	(quantitative) Polymerase chain reaction
5-AzaC	5-Azacytidine
5caC	5-Carboxylcytosine
5hmC	5-Hydroxymethylcytosine
5mC	5-Methylcytosine in DNA
ABH1 – 8	AlkB family of α-ketoglutarate and Fe(II)-dependent dioxygenases 1 – 8 in human cells
APS	Ammonium persulfate
BPTE	Bis-tris EDTA PIPES
BS	Bisulfite sequencing
BT	Bisulfite treatment
C34	Cytosine of wobble position 34 of mitochondrial tRNAs
cDNA	Complementary DNA
CDS	Coding sequence
Cp	Crossing point
CRAC	UV cross-linking and analysis of cDNA
DMEM	Dulbecco's modified eagle medium
DNA	Deoxyribonucleic acid
DNMT2	DNA methyltransferase 2
dNTPs	Deoxynucleoside triphosphates
DTT	Dithiothreitol
E. coli	*Escherichia coli*
EDTA	Ethylenediaminetetraacetic acid
f^5C	5-Formylcytosine
FCS	Fetal calf serum
FLAG	FLAG octapeptide
FTO	α-Ketoglutarate and Fe(II)-dependent dioxygenase FTO
g	Gravitational force
GFP	Green fluorescent protein

HEK 293	Human embryonic kidney 293
HeLa CCL2	Henrietta Lacks CCL2
His	Histidine
i^6A	Isopentenyladenosine
IMAC	Immobilised-metal affinity chromatography
IPTG	Isopropyl β-D-1-thiogalactopyranoside
lncRNA	Long non-coding RNA
LSU	Large ribosomal subunit
m^1A	1-Methyladenosine
m^1G	1-Methylguanosine
m^1U	1-Methyluridine
m^3C	3-Methylcytidine
m^3T	3-Methylthymidine
m^5C	5-Methylcytosine
m^6A	N6-Methyladenosine
MBP	Maltose-binding protein
$mchm^5U$	5-Methoxycarbonylhydroxymethyluridine
mcm^5U	5-Methoxycarbonylmethyluridine
MELAS	Mitochondrial encephalomyopathy, lactic acidosis, and stroke-like episode syndrome
MERRF	Myoclonic epilepsy with ragged red fibres syndrome
METTL3 and METTL14	Methyltransferase-like 3 and 14
miRNA	Micro RNA
Mitogenome	Mitochondrial genome
Mitoribosome	Mitochondrial ribosome
MLASA1	Mitochondrial myopathy, lactic acidosis and sideroblastic anaemia 1
MOPS	3-(N-morpholino)propanesulfonic acid
MRM1 – 3	Mitochondrial rRNA methyltransferase 1 – 3
mRNA	Messenger RNA
mt-mRNA	Mitochondrial mRNA
mt-rRNA	Mitochondrial rRNA

mt-tRNA	Mitochondrial tRNA
mtDNA	Mitochondrial DNA
MTERF4	Mitochondrial transcription termination factor 4
NGS	Next generation sequencing
Ni-NTA	Nickel-nitrilotriacetic acid
NSUN1 – 7	Nol1/Nop2/Sun domain family of proteins 1 – 7
NTPs	Nucleoside triphosphates
OD_{600}	Optical density at a wavelength of 600 nm
OXPHOS	Oxidative phosphorylation
PAA	Polyacrylamide
PAGE	Polyacrylamide gel electrophoresis
PBS	Phosphate-buffered saline
PCI	Phenol-chlorophorm-isoamyl alcohol
PNK	Polynucleotide kinase
Prc	PreScission protease cleavage site
PTC	Peptidyl transferase centre
PUS1	Pseudouridine synthase 1
r-RNP	Ribosomal RNP
RBFA	Ribosome-binding factor A
RBT	Reduced bisulfite treatment
RNA	Ribonucleic acid
RNA-IP	RNA immunoprecipitation
RNAi	RNA interference
RNP	Ribonucleoprotein
Rosetta	Rosetta DE3 pLysS competent cells
rpm	Rounds per minute
rRNA	Ribosomal RNA
SAM	S-Adenosyl methionine
SDS	Sodium dodecyl sulfate
siRNA	Small interfering RNA
snoRNA	Small nucleolar RNA

snoRNP	Small nucleolar ribonucleoprotein
snRNA	Small nuclear RNA
SSC	Saline-sodium citrate
SSU	Small ribosomal subunit
TAE	Tris acetic acid EDTA
TBE	Tris borate EDTA
TET	Ten-eleven translocation
TFB1M and TFB2M	Mitochondrial dimethyltransferase 1 and 2
TMI	2,3,3 Trimethylindolenin
TMN	Tris magnesium sodium
TRM4	S-Adenosyl-l-methionine-dependent m^5C-methyltransferase
TRMT1	tRNA methyltransferase 1
TRMT5	mt-tRNA methyltransferase 5
tRNA	Transfer RNA
UTR	Untranslated region
WES	Whole exome sequencing
WTAP	Wilms' tumour 1-associating protein
τm^5s^2U	5-Taurinomethyl-2-thiouridine
τm^5U	5-Taurinomethyluridine

1 Introduction

1.1 RNA modifications

1.1.1 General overview

The central dogma of molecular biology describes the flow of genetic information from deoxyribonucleic acid (DNA) to protein, mediated by ribonucleic acids (RNA) and ribonucleoprotein (RNP) complexes. DNA, located in the cell's nucleus, consists of a double-stranded chain of nucleotides, which holds the genetic information for integrity, function, development and reproduction of all living organisms. Chemical modifications of the DNA nucleobases have been found to affect transcription of DNA into RNA sequences, without affecting underlying DNA sequence. Understanding these complex "epigenetic" regulatory mechanisms has expanded our knowledge of gene expression and gene expression regulation (reviewed in Strahl and Allis 2000; Suzuki and Bird 2008).

Although chemical modifications in RNA were first detected in the 1970s, their possible role in gene expression regulation was long neglected. While modifications in DNA mostly feature methylation of cytosines or its oxidised products, chemical modifications in RNA are much more diverse and occur in different types of cellular RNA, including messenger RNA (mRNA), ribosomal RNA (rRNA) and transfer RNA (tRNA). Interestingly, recent findings also point towards an involvement in pathogenic conditions including the formation of cancer, making further research necessary (reviewed in Wang and He 2014).

1.1.2 mRNA, rRNA and tRNA modifications and their functions

Modifications are found throughout the transcriptome, which by analogy to the epigenetic modifications in DNA, has led to the introduction of the term "epitranscriptome", that includes all coding and non-coding RNA. The identification of such RNA modifications has been made possible by the development of transcriptome-wide mapping approaches for specific modifications either based on their specific chemical reactivities or on the

development of modification specific antibodies that allow specific enrichment of modification-containing RNAs for analysis by Next generation sequencing (NGS) (Helm and Motorin 2017). tRNAs and rRNAs are the most extensively modified species with 17 % and 2 % of nucleotides carrying modifications respectively. Modifications to RNA nucleotides influence their topological properties and can thereby influence the fate of the RNAs that carry them. For example, RNA modifications can influence the stability or folding of RNAs as well as their interactions with proteins (Watkins and Bohnsack 2012).

mRNAs in eukaryotic cells convey the genetic information from DNA in the nucleus to the ribosomes in cytosol. The most prominent modifications of mRNAs are the 5' cap and the poly(A) tail at the 3' end of the molecule. However, modifications are also found along the length of mRNAs. While modifications at both ends seem to level RNA synthesis, modifications within the coding sequence (CDS) of the RNA recently gained attention for their roles in mRNA metabolism and decay. Most prevalent in mRNA of higher eukaryotes is the internal modification N^6-methyladenosine (m^6A), that has been found in over 7000 mRNAs so far (reviewed in Roundtree et al. 2017). It is specifically enriched around stop codons, but is also present in 3' untranslated regions (UTRs) and in internal long exons (Dominissini et al. 2012). With an average of 3 – 5 modification sites per mRNA, it occurs on only 0.1 – 0.4 % of adenosines present (Tuck 1992). m^6A modifications in mRNA are mostly introduced co-transcriptionally by a large methyltransferase core complex formed by methyltransferase-like 3 and methyltransferase-like 14 (METTL3 and METTL14) and the mammalian splicing factor wilms' tumour 1-associating protein (WTAP) (Roundtree et al. 2017). Installed m^6A modifications can be recognised by m^6A-binding proteins that regulate gene expression by influencing splicing, translation, transcript stability and decay of target RNA (Wang et al. 2014; Wang and He 2014; Wang et al. 2015; Xiao et al. 2016).

rRNA is an essential component of the cell's protein-manufacturing machinery located either free in the cytoplasm or bound to the endoplasmatic reticulum. Each eukaryotic ribosome is composed of a small ribosomal subunit (SSU) containing one rRNA and a large ribosomal subunit (LSU) containing three rRNAs. The LSU catalyses peptide bond formation whereas the SSU decodes mRNAs which together guarantee proper enzymatic function in mRNAs

translation into proteins. The rRNA modification landscape is much less diverse compared to tRNAs or mRNAs, but the rRNAs are highly modified, with 10 diversely methylated bases, 91 pseudouridines and 105 2'-o-ribose methylations identified in the human rRNAs (Piekna-Przybylska et al. 2008).

Installation of rRNA modifications generally takes place early in the ribosome biogenesis pathway in the nucleolus and is catalysed mainly by Box C/D and H/ACA small nucleolar ribonucleoproteins (snoRNPs). These consist of a small nucleolar RNA (snoRNA) that specifically interacts with the rRNA by base-pairing of complementary snoRNA sequence with target rRNA modification site as well as protein components that are either structural or catalyse the rRNA modification. Uridine is converted to pseudouridine by H/ACA snoRNP and the 2'-hydroxyl group of the ribose is methylated by box C/D snoRNPs, respectively (Watkins and Bohnsack 2012). Interestingly, in yeast, lack of some of the modifications installed by snoRNPs affects ribosome assembly and function, implicating them as quality control checkpoints in ribosome biogenesis (Liang et al. 2007, 2009). Sites of the ribosomal RNP (r-RNP) that are functionally important, including the peptidyl transferase centre (PTC), the aminoacyl-, peptidyl- and exit-site of tRNAs binding mRNA, the polypeptide exit tunnel and the intersubunit bridges, are the areas where the rRNA is most extensively modified (Decatur and Fournier 2002). This clustering of modifications in important regions of the ribosome seems to have an influence on ribosomal structure and function. It is suggested to help preserve the three-dimensional conformational architecture of the ribosome (Davis 1995; Blanchard and Puglisi 2001; Hörbartner 2002). Studies have also shown that hypomodification of rRNAs leads to severe growth phenotypes in yeast (Tollervey et al. 1993; Zebarjadian et al. 1999). Also, peptide bond synthesising activity is decreased in prokaryotic ribosomes that were reconstituted without rRNA modifications (Green and Noller 1999; Khaitovich et al. 1999), emphasising the importance of modifications in each step of the ribosome assembly and function.

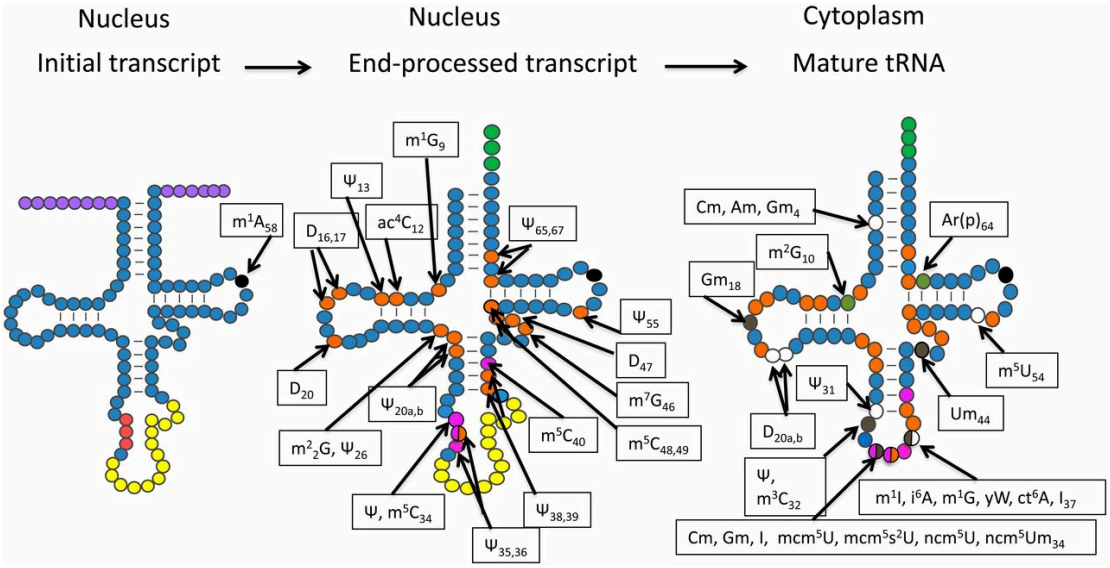

Figure 1: tRNA modifications in *Saccharomyces cerevisiae*.
RNA modifications in tRNAs excel through high diversity as well as quantity, counting approximately 85 modifications that have been found so far. These modifications include pseudouridylations and various elaborate hypermodifications, as shown above, found in baker's yeast *Saccharomyces cerevisiae*. Located primarily at the anticodon-loop, on the wobble position 34 and on position 37, and in the structural core of the tRNAs, they are in general introduced during maturation of the tRNAs and are responsible for precise codon-anticodon recognition and tRNA stability, respectively.
(Hopper 2013). With kind permission from the Genetics Society of America.

Ribosomes associate with amino acids via tRNAs that act as physical links between mRNAs and the elongating peptide chain in translation. tRNAs are the most heavily modified RNA species with numerous base methylations, pseudouridylations and various elaborate hypermodifications (Figure 1). Established by multiple enzymes, tRNA modifications and a protein component are characterised by quantity as well as high diversity, accounting for about 80 % of all RNA modifications (Sprinzl and Vassilenko 2005; El Yacoubi et al. 2012; Boccaletto et al. 2018). Installation of modifications in tRNAs primarily takes place in the nucleus or cytoplasm by lone-standing enzymes, and can be broadly classified into two groups depending on their location within the tRNA sequence. On the one hand, installed in the anticodon-loop, primarily on the wobble position 34 and on position 37, they are essential for precise mRNA-decoding. For example, modifications on position 34 can expand or focus the interactions between codons and anticodons, allowing optimal reading of the genetic code. On the other hand, tRNA modifications in the structural core of the tRNA ensure structural integrity and stability of the tRNA by promoting Watson-Crick base pairing, electrostatic interactions and magnesium-ion

binding during tRNA folding (Hall et al. 1989; Voigts-Hoffmann et al. 2007). While deletion of single modifications in the body of tRNAs often does not have a big impact on tRNA stability, hypomodification of multiple nucleotides can lead to faster degradation (Alexandrov et al. 2006).

For a long time, nucleotide modifications in tRNAs were seen as static decorations after their initial installation. Yet, recent studies hint that specific modifications also respond to environmental changes as well as metabolic alterations within the cell. One clear example has been found in yeast, where the s-adenosyl-l-methionine-dependent m^5C-methyltransferase (TRM4) modifies the wobble position of $tRNA^{Leu(CAA)}$ in cells exposed to oxidative stress, leading to increased translation of TTG-rich transcripts. As a result, translation of the ribosomal protein paralog RPL22a is enhanced, suggesting a dynamic tRNA modification of the wobble position of $tRNA^{Leu(CAA)}$ helps respond to stress and ensures cell survival (Chan et al. 2012).

1.1.3 Dynamics of RNA modifications

It recently has come to light that, similar to the U modifications on position 34 installed by TRM4, many other RNA modifications are also dynamic: Modifications in RNAs can be differentially installed by enzymes that act as “writers”, but they can also be actively removed by other enzymes termed “erasers”, creating a level of dynamics that enables cells to respond to changing conditions (Yue et al. 2015).

This level of dynamics is well characterised in case of m^6A in mRNA (Figure 2). The levels of the METTL3 has been shown to vary between cell types and in different conditions, which has been shown to lead to variations in the amount and position of m^6A modifications installed. Also, active deinstallation of m^6A by “eraser” proteins has been described. Two members of the AlkB family of α-ketoglutarate and Fe(II)-dependent dioxygenases (ABH1 – 8 and FTO in human cells), the m^6A demethylation enzymes ABH5 and FTO, oxidatively reverse m^6A in mRNA, hence altering the effects of m^6A binding proteins on regulating gene expression (Jia et al. 2011; Zheng et al. 2013).

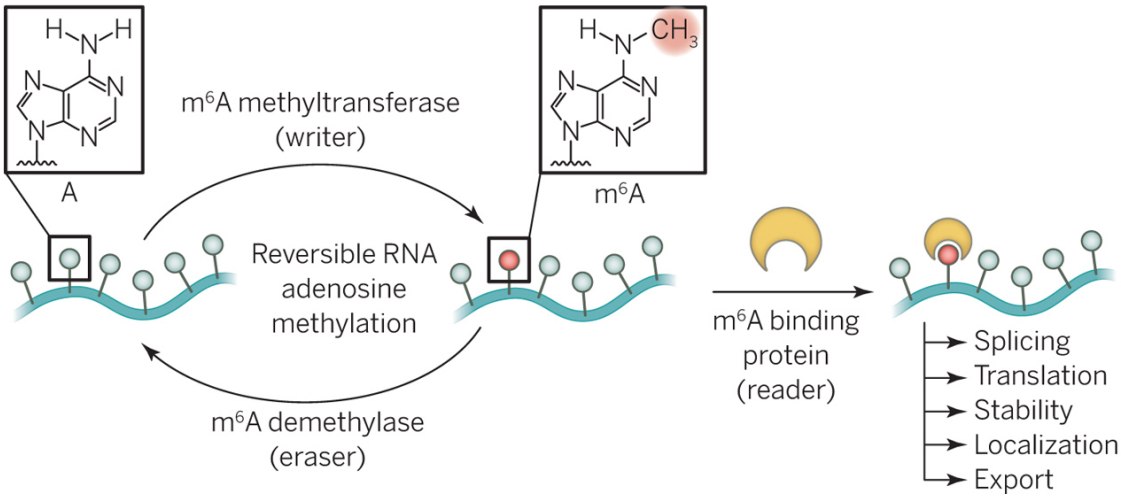

Figure 2: Dynamics of the RNA modification m^{6}A in mRNA.
In human mRNA, the reversible RNA modification N6-methyladenosine (m^{6}A) can be installed or actively remove by enzymes that act as "writers" or "erasers", respectively. m^{6}A binding proteins, that act as "readers", specifically detect the RNA modification, influencing mRNAs processing downstream including its structure and stability, localisation, export and translation. (Dominissini 2014). With kind permission from the author.

ABH proteins have been implicated in the demethylation of a variety of methylated bases in DNA but also in RNA, including 3-methylthymidine (m^{3}T), 3-methylcytidine (m^{3}C), 1-methylguanosine (m^{1}G) and 1-methyladenosine (m^{1}A). With nine homologues in the human genome, the range of substrates being described for these enzymes has increased dramatically since the initial discovery of ABH3 as an example of a DNA repair enzyme (Fedeles et al. 2015).

ABH2 and ABH3 mainly act as DNA repair enzymes and remove m^{1}A and m^{3}C modifications (Duncan et al. 2002; Ringvoll et al. 2008). ABH3 has also recently been shown to demethylate m^{3}C in RNA (Chen et al. 2018). ABH5, ABH8 and FTO all bind RNA and ABH5 and FTO also specifically oxidise m^{6}A(m) in mRNAs. In contrast, ABH8, which contains a specific RNA recognition motif, a methyltransferase domain, and an AlkB-like domain, first generates 5-methoxycarbonylmethyluridine (mcm^{5}U) using its methyltransferase domain. Then the AlkB-like domain generates 5-methoxycarbonylhydroxymethyluridine (mchm^{5}U), which is present at the wobble position of tRNAs such as tRNA$^{Gly(UCC)}$ (Fu et al. 2010; van den Born et al. 2011). Interestingly, ABH1 and ABH4 have been suggested to interact with proteins and alter the histone H2A methylation status in neuronal development (Ougland et al. 2012) and ABH4

has also been suggested to be responsible for dynamic actin demethylation during cytokinesis (Li et al. 2013). ABH1 has also been shown to demethylate m^3C and m^1A in RNA and DNA nucleosides in vitro (Westbye et al. 2008), suggesting that it is a multifunctional enzyme. Indeed, more recently, ABH1 was reported to demethylate m^1A in a number of cytoplasmatic and mitochondria (Liu et al. 2016; Kawarada et al. 2017).

1.1.4 RNA modifications and disease

New whole genome sequencing approaches enable to map disease-associated mutations in RNA modifying enzymes and highlight their possible roles in pathologic cell processes. The general principles of how RNA modifications can lead to disease are however still matter of debate (reviewed in Jonkhout et al. 2017). One possible mechanism discussed is the role of specific RNA modifications that mediate upregulation of the cell's protein synthesis under cellular stress. No modification then can lead to an impaired cell response (Patil et al. 2012 and Deng et al. 2015). Others postulate lack of specific RNA modifications that, under certain circumstances, cause increased protein synthesis and protein aggregation within the cell that can result in cellular dysfunction (Nedialkova and Leidel 2015).

Up to 50 % of all RNA modifications that have been linked to human disease so far (Figure 3) are associated with neurodegenerative diseases, which is in accordance with the observed enrichment of several RNA modifications in neuronal tissues (Paul and Bass 1998; Chi and Delgado-Olguín 2013).

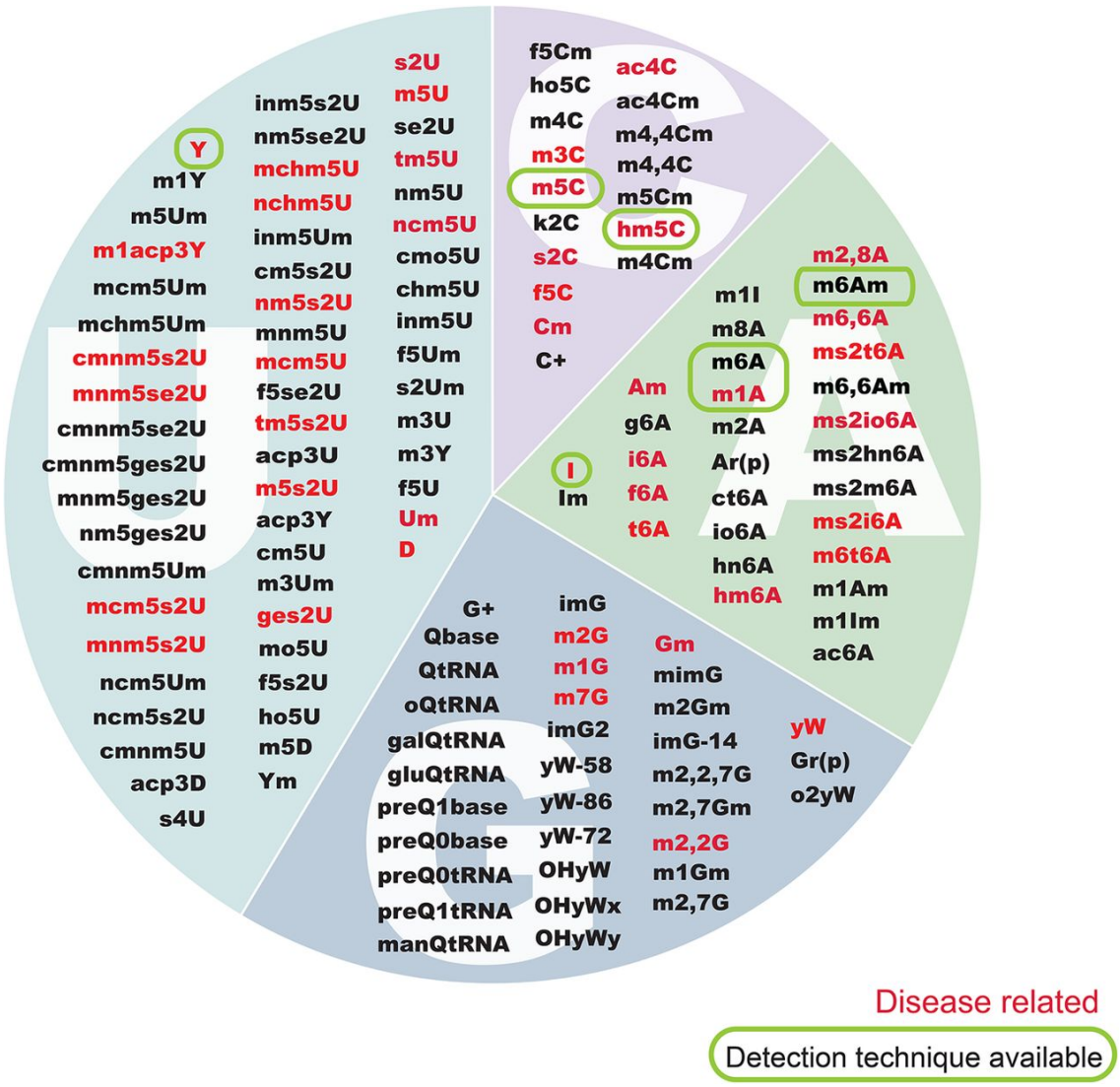

Figure 3: RNA modifications and their links to human disease.
Overview of all known RNA modifications that have been detected in human cells so far, subdivided by their reference nucleotide. Disease-related RNA modifications are marked in red. RNA modifications for which genome-wide detection methods have been established are circled in green.
(Jonkhout et al. 2017). Licensed under CC BY-NC 4.0.

In this regard, the “eraser” enzyme FTO have been found to play a critical role in the development of brain function and neurodegeneration. Developmental defects of the telencephalon and hypothalamus have been observed in mice embryos that contained a genetic deletion of the *FTO* locus, noting that FTO also oxidatively demethylates DNA.

Also, genomic variants in the *FTO* gene are associated with Alzheimer’s disease, the most common type of dementia, detecting significantly lowered expression levels of FTO. Besides, deletion of FTO seems to impair dopamine receptor control of neuronal activity in the brain and provokes behavioural

responses (Hess et al. 2013). Also, on a gene level, several RNA methyltransferase-encoding genes have been connected to intellectual disabilities (Bednářová et al. 2017), identifying tRNA methyltransferase 1 (TRMT1) to be jointly responsible for an autosomal recessive intellectual disability that clinically presents with mild to severe intellectual incapacity (Abbasi-Moheb et al. 2012; Davarniya et al. 2015).

Furthermore, mutations and dysregulation in RNA modifying enzymes have been linked to unchecked cell growth and tumorigenesis observed in several types of cancer, including prostate cancer, breast cancer and leukaemia (Tusup et al. 2018). In lung adenocarcinoma cell lines for example, high levels of m^6A have been detected. Installed by a methyltransferase complex including METTL3, METTL14 and pre-mRNA-splicing regulator WTAP, depletion of METTL3 results in decreased cancer cell growth and cell invasiveness. The methyltransferase-like 2 also seems to promote translation of certain oncogenes including the hippo pathway effector TAZ and the epidermal growth factor receptor (Lin et al. 2016). In another study, the methyltransferase Nol1/Nop2/Sun (NSUN) 2 also showed upregulation in human breast cancer cells. Tissue samples taken from breast cancer at different clinicopathological grades correlated with the overexpression of methyltransferase NSUN2 (Yi et al. 2017). Another study found NSUN2 to promote tumour growth of human gastric cancer. Interestingly, malignancy progression was effectively inhibited by knock-down of NSUN2 *in vitro* and *in vivo* (Mei et al. 2020).

Although there is no doubt that qualitative and quantitative changes in RNA modifications affect cell metabolism and cell survival, too little is known about their interplay between pathogenic mechanisms and their role in human disease. The aforementioned links between changes in RNAs modification state and human disease highlight the importance of a deeper understanding of the underlying mechanisms, and further research is needed. New drugs that specifically target RNA modifications or the enzymes that install them may become part of an integral approach of modern medicine in the diagnostic and treatment of diseases such as obesity, genetic or neurodegenerative diseases or cancer.

1.2 5-Methylcytosine and its derivatives in RNA

1.2.1 m^5C and m^5C RNA methyltransferases

A prominent example of a nucleotide modification in higher organisms is 5-methylcytosine in DNA (5mC), that alters gene expression. While it is a highly abundant well studied nucleotide modification in DNA and referred to as the "fifth base" of the human genome (Breiling and Lyko 2015), this modification also occurs in RNA.

5-methylcytosines (m^5C) can be found many in tRNAs, where m^5C sites are located around the variable region and the anticodon loop. m^5C modifications have also been detected in mRNA UTRs and near binding sites for RNA-silencing proteins that are part of the argonaute protein family (Squires et al. 2012; Song and Yi 2017). While in tRNAs, the modification helps to stabilise its secondary structure and codon recognition (Motorin and Helm 2010; Helm and Motorin 2017), in mRNAs export and post-transcriptional regulation seem to be affected by the presence of m^5C (Yang et al. 2017).

Enzymes that catalyse m^5C modifications are the seven proteins of the NSUN domain family (NSUN1 – 7) and the DNA methyltransferase 2 (DNMT2) (Bohnsack et al. 2019). DNMT2 almost exclusively targets position 38 of the $tRNA^{Asp}$ in human cells (Goll et al. 2006), whereas NSUN1 and NSUN5 catalyse rRNAs methylations (Sloan et al. 2013; Tafforeau et al. 2013; Schosserer et al. 2015), and NSUN2 and NSUN6 show specificity for tRNAs (Schaefer et al. 2010; Tuorto et al. 2012; Blanco et al. 2014; Haag et al. 2015). In mice, NSUN4 was described to be localised in mitochondria and methylate mitochondrial 12S rRNA (Cámara et al. 2011; Metodiev et al. 2014), and NSUN2 also modifies vault RNAs and mRNAs (Hussain et al. 2013).

Interestingly, NSUN2 – 7 also seem to play a role in neurocognitive development in humans, as their transcripts were found to be enriched in the developing brain (Chi and Delgado-Olguín 2013). Others could show associations to microcephaly and other neurological abnormalities in mice and humans (Frye and Watt 2006; Blanco et al. 2014; Blanco and Frye 2014). Also, mutations in the *NSUN2* gene in humans are associated with autosomal recessive forms of intellectual disability (Khan et al. 2012; Fahiminiya et al.

2014). The Dubowitz-like syndrome, another autosomal recessive disorder that clinically presents with mild microcephaly, growth and mental retardation, eczema and peculiar facies, also is associated with splice mutations in the NSUN2 gene (Martinez et al. 2012). These studies highlight the scientific and medical relevance of m^5C and the need for detailed characterisation of the enzymes that can install it.

1.2.2 5-Formylcytosine in tRNA

In DNA, it has been recently discovered that 5mC-marks can be oxidised in a stepwise fashion, first to 5-hydroxymethylcytosine (5hmC) and then to 5-formylcytosine (f^5C) and 5-carboxylcytosine (5caC) by the ten-eleven translocation (TET) family of dioxygenases, followed by passive removal either in a base excision repair mechanism by DNA glycosylases or during DNA replication (Tahiliani et al. 2009; He et al. 2011; Ito et al. 2011).

Remarkably, the f^5C intermediate, which in DNA was detected as oxidative product of 5mC through 5hmC, was first found as a stable modification in human RNA. Located at the cytosine of wobble position 34 (C34) of the mitochondrial tRNA (mt-tRNA) methionine, the chemical modification was suspected to affect codon-anticodon interaction (Moriya et al. 1994). However, at the time this study was conducted, the enzymes that install f^5C in RNA still were not known.

1.3 Cellular roles of mitochondria

Mitochondria, membrane-bound organelles located within the cell's cytoplasm, are the cells "power-houses". It is thought that two billion years ago, an aerobic prokaryotic cell made its way inside an ancestral eukaryotic cell by endocytosis and the advantage conferred by its ability to produce energy lead to it being retained through evolution, thus giving rise to mitochondria (reviewed in Lang et al. 1999).

In addition to being the main energy supplier in eukaryotic cells by oxidative phosphorylation (OXPHOS), mitochondria are involved in several other metabolic tasks, including steroid hormone synthesis, breakdown of fatty acids, certain haeme synthesis reactions, calcium signalling, but also tissue-

dependent tasks, for example hormonal signalling in brain cells. In human pathology and ageing, mitochondrial functioning is vital, and dysfunction can be associated with several disease like heart failure, autism and depression (Oh-hama 1997; Gardner and Boles 2005; McBride et al. 2006; Napoli et al. 2014; Dorn et al. 2015).

1.3.1 Mitochondrial translation

In all eukaryotic cells, mitochondrial proteins derive from two sources: First, mRNAs encoding the vast majority of all approximately 3000 proteins present in mitochondria are transcribed from nuclear DNA. Cytoplasmic-translated protein precursors are therefore imported over the phospholipid bilayer of mitochondria by protein translocases into the mitochondrial matrix. Secondly, mitochondrial proteins can be produced by the mitochondria's own protein machinery. This differs from its cytoplasmic counterpart as all mRNAs are transcribed from mitochondrial DNA (mtDNA) and translated into proteins on mitochondrial ribosomes (mitoribosomes) by use of an alternative genetic code (Mokranjac and Neupert 2005; Hällberg and Larsson 2014).

The mitochondrial genome (mitogenome), present in multiple copies in the mitochondrial matrix, consists of a double-stranded circular mtDNA. In humans it encodes 13 mRNAs whose protein products all are components of OXPHOS, 22 mitochondrial transfer RNAs (mt-tRNAs) and two mitochondrial ribosomal RNAs (mt-rRNAs) (Anderson et al. 1981; Ott et al. 2016). Given that all genetic information of mtDNA is essential for proper mitochondrial function, mitochondrial protein synthesis is tightly regulated and is carefully balanced with expression of nuclear-encoded proteins (Neupert 2016).

As mitochondria only express a minimal set of only 22 tRNAs, brought to the 55S mitoribosome by translation factors similar to prokaryotic translation system, the mitochondrial translation machinery differs from the canonical decoding system by following a non-conventional code. In comparison to conventional cytosolic translation initiation by start codon AUG, mitochondria’s non-conventional genetic code additionally makes use of the start codons AUA and AUU. In contrast to bacterial and cytosolic translation, these three codons are all decoded by a single mt-tRNA^{Met}, which functions during both translation initiation and elongation. In mitochondrial translation termination, the stop

codons UAA, UAG, AGA and AGG are used instead of the cytosolic UAA, UAG and UGA ones (reviewed in Anderson et al. 1981).

In total, 60 sense codons are decoded by a set of only 22 mt-tRNAs. The wobble position, which is the first position of the tRNAs anticodon, basepairs with the third position of the mRNA codon, therefore plays a key role in mitochondria. By not following Watson-Crick base pair rules and carrying diverse modifications, the tRNA wobble base can form non-standard base pairings with the mRNA's codon sequence, hence expanding the codon-anticodon combinations that can be used during translation (reviewed in Suzuki et al. 2011).

1.3.2 Mitochondrial RNA modifications

Mitoribosomes contain two mt-rRNAs that are much less modified in comparison to their bacterial and cytoplasmic counterparts, with only ten modification sites that have been detected so far (Rorbach and Minczuk 2012; Bar-Yaacov et al. 2017). Current data from Single-particle cryo-electron microscopy of the mammalian mitoribosome showed that the modified nucleotides would be present at functionally important regions, namely the decoding centre of the SSU or the PTC located in the LSU (Amunts et al. 2015).

Mitochondrial dimethyladenosine transferase 1 and 2 (TFB1M and TFB2M) were the first enzymes discovered to install RNA modifications in mt-rRNA. By installation of two adenosine dimethylations ($m^6{}_2A$) close to the 3'-end of the 12S rRNA, the s-adenosyl methionine (SAM)-dependent methyltransferases enable binding of ribosome-binding factor A (RBFA), maintaining translation efficiency. Studies also found decreased stability of the SSU in absence of RBFA (Lafontaine et al. 1998; Shutt and Shadel 2010; Rozanska et al. 2017). The methyltransferase NSUN4, another enzyme to install RNA modifications in mt-rRNA, seems to act on both mitoribosomal subunits. While it installs m^5C at position 841 of the SSU, together with mitochondrial transcription termination factor 4 (MTERF4), it is also involved in the assembly of the LSU. This dual function, also reported for several RNA methyltransferases (van Nues et al. 2011; Falaleeva et al. 2016; Jorjani et al. 2016; Sloan et al. 2017), may imply a mechanism for coordinated maturation of the two ribosomal subunits (Cámara et al. 2011; Spåhr et al. 2012; Metodiev et al. 2014). Other mt-rRNA

modifications found in the LSU are three 2'-O-methylations installed by the mitochondrial rRNA methyltransferases 1 – 3 (MRM1 – 3), respectively, close to the functionally important Aminoacyl-, and Peptidyl-sites of the PTC (Lee et al. 2013; Lee and Bogenhagen 2014; Rorbach et al. 2014).

While cytosolic tRNAs carry a large number of RNA modifications, in the 22 mammalian mt-tRNAs, in contrast, RNA modifications are much sparser, with only 15 different types at 118 positions identified so far. Installed by nuclear, cytoplasmic-derived enzymes, modifications such as m^5C, f^5C and most abundant, pseudouridylation, ensure mt-tRNA stability and function (Suzuki and Suzuki 2014). The multifunctional enzyme pseudouridine synthase 1 (PUS1), that also installs modifications in cytoplasmic tRNAs, has been identified to guide pseudouridylation in mt-tRNAs. It is hypothesised that these modifications have a strong stabilising effect on the secondary structure due to its greater hydrogen bonding potential after isomerisation of U to pseudouridine (Patton et al. 2005).

Positions 34 and 37 are two modification hotspots of mt-tRNAs, that are of high importance as they are responsible for maintaining decoding flexibility. 60 mitochondrial mRNA (mt-mRNA) codons are read by minimal set of only 22 mt-tRNAs. Thus, these anticodon loop bases undergo heavy modification and hypermodification to regulate codon selection and anticodon-codon interaction (Suzuki 2005; El Yacoubi et al. 2012).

Position 37 was found to carry several different types of modifications in human mt-tRNAs, including methylations, and especially complex hypermodifications. The mt-tRNA methyltransferase 5 (TRMT5) installs 1-methyluridine (m^1U) in mt-tRNA$^{Leu(CUN)}$, mt-tRNA^{Pro} and mt-tRNA^{Gln}, which is suggested to prevent frameshifting errors in translation. Reduction of Watson-Crick basepairing induced by the presence of this modification may lead to reduced interactions with nearby mt-tRNA nucleotides and impede erroneous mt-mRNA interactions (Urbonavicius et al. 2001; Brulé et al. 2004; Powell et al. 2015). One of the first hypermodifications on position 37 to be found was the methylthiolation (ms^2i^6A) of isopentenyladenosine (i^6A) of four mt-tRNAs. Installed by isopentenyl transferase enzymes, the hypermodification has been reported to stabilise

adenine to uracil basepairing and affect speed of translation in bacteria and eukaryotes (Söll 1971; Persson et al. 1994; Grosjean and Westhof 2016).

Interestingly, there has been found only four different types of modified nucleotides at position 34 of mammalian mt-tRNAs so far. Queuosine in mt-tRNAs that carry the amino acids asparagine, aspartate, histidine and tyrosine, the taurine-modifications 5-taurinomethyl-2-thiouridine (τm^5s^2U) and 5-taurinomethyluridine (τm^5U) installed in mt-tRNAs that carry glutamine, glutamate, leucine, lysine and tryptophan and f^5C, that is found exclusively in mt-$tRNA^{Met}$. In case of f^5C, the exact modification pathway and corresponding enzymes responsible for the installation of this modification were unknown at the time this study was conducted (Suzuki and Suzuki 2014; Bohnsack and Sloan 2018).

1.3.3 Mitochondrial RNA modifications and disease

Due to the fact that modifications of mitochondrial RNAs seem to play an important role in mitochondrial homeostasis, it is reasonable that defects in enzymes installing mt-RNA modifications can compromise mitochondrial function. Impaired mt-RNA modifications have their origin either from mutations of RNA modification enzymes that come from the nucleus, or from mutations that occur in mtDNA encoding mt-rRNAs and mt-tRNAs.

For example, TFB1M is involved in several diseases. Rs950994, a common variant of *TFB1M* gene in humans is associated with reduced insulin secretion in energy-demanding pancreatic islet cells, leading to elevated postprandial glucose levels and future risk of Type 2 diabetes mellitus (Metodiev et al. 2009; Koeck et al. 2011). Also, in Mitochondrial myopathy, lactic acidosis and sideroblastic anaemia 1 (MLASA1), a rare mitochondrial disorder that primary manifests with myopathy, lactic acidosis and sideroblastic anaemia, a missense mutation in the nuclear gene encoding PUS1 is assumed to be responsible. Interestingly, this mutation leads to enzymatically inactive PUS1, and lack of pseudouridylation in several mt-tRNAs has been detected (Carlile et al. 2014). Consistent with this, a knock-out mouse model of *PUS1* showed alterations in cell metabolism and reduced exercise capacity, primarily affecting energy-consuming tissue like skeletal muscle fibers (Patton et al. 2005; Carlile et al. 2014; Mangum et al. 2016).

Two diseases that have been linked to mutations in mtDNA encoding mt-tRNA are Mitochondrial encephalomyopathy, lactic acidosis, and stroke-like episode (MELAS) and Myoclonic epilepsy with ragged red fibres (MERRF). In both syndromes, defective mt-tRNA modifications (τm^5U on position 34 of mt-tRNA$^{Leu(UUR)}$ in MELAS and τm^5s^2U on position 34 of mt-tRNA^{Lys} in MERRF) have been implicated to be responsible for impaired mitochondrial function (of the respiratory chain), and even serve as the pathogenic basis in case of MELAS (Goto et al. 1990; Kobayashi et al. 1990; Kirino et al. 2005). The importance of the two mt-tRNA anticodon stem loop modifications τm^5U and τm^5s^2U on position 34 has been further underlined recently. Mutations in *MTO1* and *GTPBP3* encoding for proteins that catalyse the installation of the modifications caused mitochondrial malfunction and other metabolic entities such as Lactic acidosis (Ghezzi et al. 2012; Baruffini et al. 2013; Kopajtich et al. 2014).

1.4 Aim of the thesis

Base modifications on position 34 of mt-tRNAs, located at the anticodon stem loop, are important as they allow the translation of all codons with a minimal set of only 22 mt-tRNAs. Therefore, the so-called “wobble base” is critical for controlling codon-anticodon interaction and changes in the modification status at this position are associated with human diseases. In case of initiator and elongator tRNA mt-tRNA^{Met}, a f^{5}C has been detected at the C34-position. In this context, data of the Bohnsack lab showed that the methyltransferase NSUN3 interacts with mt-tRNA^{Met} and methylates C34. Methylated nucleosides can be subject to further modification and members of the AlkB dioxygenase family of proteins ABH1 – 8 and FTO have been shown to oxidise these modifications in DNA and RNA. Based on the known localisation to mitochondria, I hypothesised that the dioxygenase ABH1 might be responsible for the installation of f^{5}C in mt-tRNA^{Met}.

This study therefore aimed to:

- Determine if ABH1 interacts with mt-tRNA^{Met} in human cells
- Recombinantly express ABH1 and catalytically inactive mutants in *Escherichia coli* (*E. coli*) and purify the protein for use in *in vitro* oxidation and methylation assays
- Determine if purified ABH1 can convert m^{5}C to f^{5}C on synthesised RNAs *in vitro*
- Establish depletion of ABH1 in human embryonic kidney 293 (HEK 293) and Henrietta Lacks CCL2 (HeLa CCL2) human cervical carcinoma cells
- Monitor the modification status of C34 of mt-tRNA^{Met} in cells expressing or lacking ABH1

2 Materials and Methods

2.1 Materials

2.1.1 Devices, consumables and chemicals

Table 1: Devices and equipment

Product	Company
Agarose gel chamber	Bio-Rad (Hercules, USA)
Autoclave	Systec (Linden, Germany)
Bunsen burner (1430)	Usbeck (Radevormwald, Germany)
Cell incubator (Heracell 150I)	Thermo Fisher Scientific (Waltham, USA)
Centrifuge (5415 C, 5417 R and 5424)	Eppendorf (Hamburg, Germany)
Electrophoresis casting chamber (Trans-blot)	Bio-Rad (Hercules, USA)
Fluorometer (Qubit 2.0)	GE Healthcare (Chalfont St Giles, UK)
Geiger counter (LB 122)	Berthold (Bad Wildbad)
Haemocytometer counting chamber	Celeromics (Grenoble, France)
Heat block (5436)	Eppendorf (Hamburg, Germany)
Heat block (MKR 13 and TH 21)	Ditabis (Pforzheim, Germany)
Heating bath (SV 1422)	Memmert (Schwabach, Germany)
Ice machine	Ziegra Eismaschinen (Isernhagen, Germany)
Incubator (Certomat BS-1)	Sartorius (Goettingen, Germany)
Magnetic stirrer (Ika-Combimag)	Janke und Kunkel (Staufen, Germany)
Microscope (CK 40)	Olympus (Tokyo, Japan)
Microscope (ID 03)	Zeiss (Goettingen, Germany)
Microwave (MW 7804)	Severin (Sundern, Germany)
Milli-Q water purificator	SG (Barsbuettel, Germany)
Mini gel electrophoresis kit (Mini protean tetra)	Bio-Rad (Hercules, USA)
Mixer (Variomag)	Thermo Fisher Scientific (Waltham, USA)
Orbital shaker (3015)	GFL (Burgwedel, Germany)

Product	Company
Petriturn-M	Schuett Biotec (Goettingen, Germany)
Phosphoimager (Typhoon 9500)	GE Life Sciences (Chalfont St Giles, UK)
Pipettes (Research2100; 10, 20, 200 and 1000 µl)	Eppendorf (Hamburg, Germany)
Pipetting controller (Pipetboy)	Integra Biosciences (Zizers, Switzerland)
Polyacrylamide (PAA) gel chamber	Bio-Rad (Hercules, USA)
Polymerase chain reaction (PCR) machine (Flex Cycler 2)	Analytik Jena (Jena, Germany)
Power supply (1000/500 and 301)	Bio-Rad (Hercules, USA)
Quantitative (q)PCR machine (Light Cycler 480II /96)	Roche (Basel, Switzerland)
Scale (ED224S)	Sartorius (Goettingen, Germany)
Scanner (V750 pro)	Epson (Suwa, Japan)
Scintillation counter (Beckman LB 6500 IC/TA/LL)	GMI (Ramsey, USA)
Shaker (TL 10)	Edmund Bühler (Hechingen, Germany)
Shaker (Vortex Genie 2)	Scientific Industries (San Francisco, USA)
Shaking hybridization oven (3032 C and 7601)	GFL (Burgwedel, Germany)
Sodium dodecyl sulfate (SDS)-polyacrylamide gel electrophoresis (PAGE) gel chamber	Bio-Rad (Hercules, USA)
Spectrophotometer (Type SmartSpec plus)	Bio-Rad (Hercules, USA)
UV crosslinker (Stratalinker 2400)	Stratagene (La Jolla, USA)
UV table	Uvitec (Cambridge, UK)
UV transluminator (U1T-30M-83)	Biostep (Burkhardtsdorf, Germany)
Vacuum gel dryer (Dry-dryer)	Biotec-Fischer (Reiskirchen, Germany)
Vacuum pump (HydroTech)	Bio-Rad (Hercules, USA)
Water bath	GFL (Burgwedel, Germany)
Whatman cellulose filter paper	Sigma (St. Louis, USA)

Table 2: Consumables

Product	Company
Chromatography columns (10 ml)	GE Healthcare (Chalfont St Giles, UK)
Cover slips	GE Healthcare (Chalfont St Giles, UK)

Cuvettes (1, 5 and 10 ml)	Sarstedt AG & Co. (Nuembrecht, Germany)
Dry spectra regenerated cellulose membrane	Repligen (Ravensburg, Germany)
Eppendorf cups (0.2, 1.5 and 2 ml)	Sarstedt AG & Co. (Nuembrecht, Germany)
Hybond-N nylon membrane	Amersham Plc (Amersham, UK)
Microscope slides	Th. Geyer (Renningen, Germany)
Parafilm	Bemis (Neenah, USA)
PCR tubes	Brand (Wertheim, Germany)
Petri dishes (6 and 10 cm^2)	Sarstedt AG & Co. (Nuembrecht, Germany)
Pipette tips	Eppendorf (Hamburg, Germany)
Real-Time PCR 96-well plates	Roche (Basel, Switzerland)
Scintillation vials	Sarstedt AG & Co. (Nuembrecht, Germany)
Tubes (10, 15 and 50 ml)	Sarstedt AG & Co. (Nuembrecht, Germany)
X-ray film	Foma Bohemia (Hradec Králové, Czech)

Table 3: Chemicals and kits

Product	Company
3-(N-morpholino)propanesulfonic acid (MOPS) buffer	Merck (Darmstadt, Germany)
^{3}H-SAM	Perkin Elmer (Waltham, USA)
Acetic acid	Carl Roth (Karlsruhe, Germany)
Acrylamide (30 % and 40 %)	Carl Roth (Karlsruhe, Germany)
Agar-agar	PanReac AppliChem (Darmstadt, Germany)
Agarose ultrapure	Invitrogen (Carlsbad, USA)
Aluminium sulfate	PanReac AppliChem (Darmstadt, Germany)
Ammonium iron(II) sulfate	Sigma (St. Louis, USA)
Ammonium persulfate (APS)	PanReac AppliChem (Darmstadt, Germany)
Ampicillin	Carl Roth (Karlsruhe, Germany)
Anti-FLAG M2 magnetic beads	Sigma (St. Louis, USA)
Ascorbic acid	Carl Roth (Karlsruhe, Germany)
Bacto-trypton	PanReac AppliChem (Darmstadt, Germany)
Bis-tris	Carl Roth (Karlsruhe, Germany)
Boric acid	Carl Roth (Karlsruhe, Germany)

Product	Company
Bovine IgG dilutions	Sigma (St. Louis, USA)
Bradford reagent	Thermo Fisher Scientific (Waltham, USA)
Bromophenol blue	Carl Roth (Karlsruhe, Germany)
Chloramphenicol	Sigma (St. Louis, USA)
Chloroform	PanReac AppliChem (Darmstadt, Germany)
Colloidal coomassie	PanReac AppliChem (Darmstadt, Germany)
Complete his-tag purification resin	Roche (Basel, Switzerland)
Complete mini protease inhibitor cocktail	Roche (Basel, Switzerland)
Coomassie dye	Bio-Rad (Hercules, USA)
Deoxynucleoside triphosphates (dNTPs)	Thermo Fisher Scientific (Waltham, USA)
Dithiothreitol (DTT)	PanReac AppliChem (Darmstadt, Germany)
DNA oligonucleotides	Thermo Fisher Scientific (Waltham, USA)
DNA protection buffer	Bohnsack lab
DpnI restriction enzyme	Thermo Fisher Scientific (Waltham, USA)
Dulbecco's modified eagle medium (DMEM)	Thermo Fisher Scientific (Waltham, USA)
EpiTect bisulfite kit	Qiagen (Hilden, Germany
Ethylenediaminetetraacetic acid (EDTA)	PanReac AppliChem (Darmstadt, Germany)
EtOH	Carl Roth (Karlsruhe, Germany)
FastAP thermosensitive ap	Thermo Fisher Scientific (Waltham, USA)
Fetal calf serum (FCS)	Merck (Darmstadt, Germany)
First strand buffer (5 x)	Invitrogen (Carlsbad, USA)
Formamide	Carl Roth (Karlsruhe, Germany)
Genamp100 amplify fluorographic reagent	Sigma (St. Louis, USA)
GeneRuler 1 kb DNA ladder	Thermo Fisher Scientific (Waltham, USA)
Glutamine	Thermo Fisher Scientific (Waltham, USA)
Glycerol	PanReac AppliChem (Darmstadt, Germany)
Glycogen	Thermo Fisher Scientific (Waltham, USA)
Glyoxal loading dye	Sigma (St. Louis, USA)
Guanidine HCl	Sigma (St. Louis, USA)
HEPES buffer	Carl Roth (Karlsruhe, Germany)

Product	Company
HindIII restriction enzyme	Thermo Fisher Scientific (Waltham, USA)
Illumina adapters and spin columns	Illumina (San Diego, USA)
Imidazole	Carl Roth (Karlsruhe, Germany)
Isoamylalcohol	Carl Roth (Karlsruhe, Germany)
Isopropanol	PanReac AppliChem (Darmstadt, Germany)
Isopropyl β-D-thiogalactopyranoside (IPTG)	Thermo Fisher Scientific (Waltham, USA)
Kanamycin	Carl Roth (Karlsruhe, Germany)
KCl	Carl Roth (Karlsruhe, Germany)
KH_2HPO_4	Carl Roth (Karlsruhe, Germany)
KPi (pH 7.3)	Carl Roth (Karlsruhe, Germany)
Ligase buffer (10 x)	Sigma (St. Louis, USA)
Lipofectamine RNAiMax	Thermo Fisher Scientific (Waltham, USA)
Lumasafe plus scintillation liquid	Lumac Lsc (Perstorp, Schweden)
Methanol	Carl Roth (Karlsruhe, Germany)
$MgCl_2$	Carl Roth (Karlsruhe, Germany)
Micro bio-spin chromatography columns	Bio-Rad (Hercules, USA)
Mini quick spin columns	Sigma (St. Louis, USA)
Mini quick spin RNA columns	Roche (Basel, Switzerland)
Na_2HPO_4	Carl Roth (Karlsruhe, Germany)
NaAc	Carl Roth (Karlsruhe, Germany)
$NaBH_4$	Sigma (St. Louis, USA)
NaCl	Carl Roth (Karlsruhe, Germany)
NcoI	Thermo Fisher Scientific (Waltham, USA)
Nickel-nitrilotriacetic acid (Ni-NTA) slurry	Qiagen (Hilden, Germany)
Nitric oxide	University Medical Centre (Goettingen, Germany)
NP-40	Roche (Basel, Switzerland)
Nucleoside Triphosphates (NTPs)	Roche (Basel, Switzerland)
Nucleospin gel and PCR clean-up kit	Macherey-Nagel (Dueren, Germany)
Nucleospin plasmid kit	Macherey-Nagel (Dueren, Germany)
OptiMEM reduced serum media	Thermo Fisher Scientific (Waltham, USA)

Product	Company
Penicillin	Carl Roth (Karlsruhe, Germany)
Phenol	Carl Roth (Karlsruhe, Germany)
Phenol-chlorophorm-isoamyl alcohol (PCI)	Carl Roth (Karlsruhe, Germany)
Phosphate buffer for cell cultures	Thermo Fisher Scientific (Waltham, USA)
Phosphoric acid	Carl Roth (Karlsruhe, Germany)
Phusion HF buffer pack	Thermo Fisher Scientific (Waltham, USA)
Phusion HF DNA polymerase	Thermo Fisher Scientific (Waltham, USA)
PIPES buffer	Sigma (St. Louis, USA)
PreScission protease	Thermo Fisher Scientific (Waltham, USA)
Proteinase K	Roche (Basel, Switzerland)
Reverse transcriptase (Superscript II)	Invitrogen (Carlsbad, USA)
Reverse transcriptase (Superscript III)	Invitrogen (Carlsbad, USA)
Ribolock RNase inhibitor	Fermentas, Thermo Fisher Scientific (Waltham, USA)
RNase-free H_2O	Qiagen (Hilden, Germany)
S.O.C. media	Thermo Fisher Scientific (Waltham, USA)
Safeview nucleic acid stain	NBS Biologicals (Huntingdon, UK)
SAM	Sigma (St. Louis, USA)
SDS	Carl Roth (Karlsruhe, Germany)
SDS-PAGE Loading dye (5 x)	Thermo Fisher Scientific (Waltham, USA)
Sodium citrate	Carl Roth (Karlsruhe, Germany
Sodium phosphate	Carl Roth (Karlsruhe, Germany)
Streptomycin	Fermentas, Thermo Fisher Scientific (Waltham, USA)
SYBR-Mix	Thermo Fisher Scientific (Waltham, USA)
T4 DNA ligase	Sigma (St. Louis, USA)
T4 PNK buffer A (10 x)	Thermo Fisher Scientific (Waltham, USA)
T4 Polynucleotide kinase (PNK)	Thermo Fisher Scientific (Waltham, USA)
T7 RNA polymerase	Sigma (St. Louis, USA)
Tango buffer	Thermo Fisher Scientific (Waltham, USA)
Taq polymerase and buffer (10 x)	Bohnsack lab
Tetracycline	PanReac AppliChem (Darmstadt, Germany)

Product	Company
Tetramethylethylenediamine (TEMED)	Carl Roth (Karlsruhe, Germany)
TOPO TA cloning kit	Thermo Fisher Scientific (Waltham, USA)
Transcription buffer (5 x)	Thermo Fisher Scientific (Waltham, USA)
Tris and Tris-HCl	Carl Roth (Karlsruhe, Germany)
Trizol Reagent	Sigma (St. Louis, USA)
Trypsin	Thermo Fisher Scientific (Waltham, USA)
Trypsin-EDTA	Thermo Fisher Scientific (Waltham, USA)
Turbo DNase	Carl Roth (Karlsruhe, Germany)
Turbo DNase buffer	Carl Roth (Karlsruhe, Germany)
Urea	Sigma (St. Louis, USA)
Whatman paper	Amersham Plc (Amersham, UK)
Xylene cyanole	Carl Roth (Karlsruhe, Germany)
Yeast extract	Carl Roth (Karlsruhe, Germany)
α-Ketoglutarate	Sigma (St. Louis, USA)
β-Mercaptoethanol	Carl Roth (Karlsruhe, Germany)
γ-[32P]-ATP	Perkin Elmer (Waltham, USA)

2.1.2 Buffers and solutions

All regularly used buffers are abbreviated as follows: bis-tris EDTA PIPES (BPTE) buffer, immobilised-metal affinity chromatography (IMAC) buffers, nickel-nitrilotriacetic acid (Ni-NTA) washing buffers, phosphate-buffered saline (PBS) buffer, saline-sodium citrate (SSC) buffer, tris acetic acid EDTA (TAE) buffer, tris borate EDTA (TBE) buffer, Tris magnesium sodium (TMN) buffers.

Table 4: BPTE buffer (10 x)

Components	Final concentration
Bis-tris	300 mM
EDTA	0.5 M
PIPES buffer	100 mM

Table 5: Coomassie staining solution

Components	Final concentration
Acetic acid	10 %
Coomassie brilliant blue	1.2 mM
Methanol	50 %

Table 6: Colloidal coomassie staining solution

Components	Final concentration
Coomassie staining solution	
Aluminium sulfate	5 %
Phosphoric acid	2 %

Table 7: Dialysis buffer I

Components	Final concentration
DTT	1 mM
EDTA	0.1 mM
Glycerol	20 %
KCl	200 mM
KPi (pH 7.3)	30 mM

Table 8: Dialysis buffer II

Components	Final concentration
DTT	1 mM
EDTA	0.1 mM
Glycerol	50 %
KCl	100 mM
KPi (pH 7.3)	30 mM

Table 9: Fixing solution

Components	Final concentration
Acetic acid	10 %
Methanol	10 %

Table 10: High stringency buffer

Components	Final concentration
SSC buffer (2 x)	
SDS	0.1 %

Table 11: IMAC elution buffer

Components	Final concentration
DTT	0.1 mM
Glycerol	10 %
Imidazole	300 mM
KCl	300 mM
KPi (pH 7.3)	30 mM

Table 12: IMAC washing buffer

Components	Final concentration
DTT	0.1 mM
Glycerol	10 %
Imidazole	10 mM
KCl	300 mM
KPi (pH 7.3)	30 mM

Table 13: Laemmli buffer

Components	Final concentration
Bromophenol blue	0.002 %
Glycerol	10 %
SDS	4 %
Tris (adjust to pH 6.8)	625 mM

Table 14: Methylation buffer (10 x)

Components	Final concentration
DTT	1 mM
NaCl	50 mM
$MgCl_2$	5 mM
Tris (adjust to pH 7.7)	50 mM

Table 15: $NaBH_4$ solution

Components	Final concentration
KCl	400 mM
$MgCl_2$	40 mM
$NaBH_4$	500 mM
Tris (adjust to pH 7.5)	400 mM

Table 16: Ni-NTA washing buffer I

Components	Final concentration
Guanidine HCl	6 M
Imidazole	10 mM
NaCl	300 mM
NP-40	0.1 %
Tris-HCl (adjust to pH 7.8 at 4 °C)	50 mM
β-Mercaptoethanol (freshly added)	5 mM

Table 17: Ni-NTA washing buffer II

Components	Final concentration
Imidazole	10 mM
NaCl	50 mM
NP-40	0.1 %
Tris-HCl (adjust pH 7.8 at 4 °C)	50 mM
β-Mercaptoethanol (freshly added)	5 mM

Table 18: Ni-NTA washing buffer III

Components	Final concentration
Ni-NTA washing buffer II	400 µl
EDTA	5 mM
SDS	1 %

Table 19: Oxidation buffer

Components	Final concentration
Ascorbic acid	4 mM
HEPES buffer	50 mM
$MgCl_2$	5 mM
Ammonium iron(II) sulfate (freshly added)	100 µM
α-Ketoglutarate (freshly added)	100 µM

Table 20: PBS buffer (10 x)

Components	Final concentration
NaCl	1.37 M
KCl	27 mM
Na_2HPO_4	80 mM
KH_2PO_4	15 mM

Table 21: Phosphate buffer (10 mM)

Components	Final concentration
KCl	2.7 mM
KH_2HPO_4	2 mM
Na_2HPO_4	10 mM
NaCl	137 mM

Table 22: Pre-hybridisation buffer

Components	Final concentration
EDTA	1 mM
SDS	7 %
Sodium phosphate	0.5 M

Table 23: PreScission eluate buffer

Components	Final concentration
Guanidine HCl	6 M
Imidazole	10 mM
NaCl	300 mM

Table 24: RNA loading dye

Components	Final concentration
Bromophenol blue	0.1 %
EDTA	5 mM
Formamide	95 %
Xylene cyanole	0.1 %

Table 25: Sonication buffer

Components	Final concentration
Complete mini protease inhibitor cocktail	1 tablet
NaCl	150 mM
NP-40	0.1 %
Tris-HCl (adjust to pH 7.6)	50 mM
β-Mercaptoethanol	5 mM

Table 26: SSC buffer (20 x)

Components	Final concentration
NaCl	3 M
Sodium citrate (adjust to pH 7.0 with HCl)	0.3 M

Table 27: TAE buffer (50 x)

Components	Final concentration
Acetic acid	1 M
EDTA	50 mM
Tris	2 M

Table 28: TBE buffer (10 x)

Components	Final concentration
Boric acid	2 mM
EDTA	2 mM
Tris	89 mM

Table 29: TMN 150 buffer

Components	Final concentration
NaCl	150 mM
NP40	0.1 %
$MgCl_2$	1.5 mM
Tris-HCl	50 mM
β-Mercaptoethanol (freshly added)	9 mM

Table 30: TMN 1000 buffer

Components	Final concentration
NaCl	1 M
NP40	0.1 %
$MgCl_2$	1.0 mM
Tris-HCl	50 mM
β-Mercaptoethanol (freshly added)	9 mM

2.1.3 Cell lines and cell culture media

Table 31: Eukaryotic cell lines

Cell line	Company
HEK 293 cells	Thermo Fisher Scientific (Waltham, USA)
HeLa CCL2 cells	Thermo Fisher Scientific (Waltham, USA)
One shot TOP10 chemically competent *E. coli*	Thermo Fisher Scientific (Waltham, USA)
Rosetta DE3 pLysS competent (rosetta) cells	Merck (Darmstadt, Germany)

Table 32: Lysogeny broth media solution

Components	Final concentration
Milli-Q H_2O	
Bacto-trypton	10 g/l
NaCl	55 g/l
Yeast extract	5 g/l

Table 33: Lysogeny broth agar

Components	Final concentration
Lysogeny broth media solution	
Agar-agar	13 g/l

Table 34: Lysogeny broth amp-agar

Components	Final concentration
Lysogeny broth media solution	
Agar-agar	13 g/l
Ampicillin	50 µg/ml

Table 35: Lysogeny broth amp-can media

Components	Final concentration
Lysogeny broth media solution	
Ampicillin	50 µg/ml
Kanamycin	10 µg/ml

Table 36: Lysogeny broth kan-agar

Components	Final concentration
Lysogeny broth media solution	
Agar-agar	13 g/l
Kanamycin	10 µg/ml

Table 37: HEK 293 cell lines for expression of HisPrcFLAG- tagged dioxygenases

Components	Source
ABH1-HisPrcFLAG* (ABH1)	
ABH2-HisPrcFLAG* (ABH2)	
ABH3-HisPrcFLAG* (ABH3)	Bohnsack
ABH4-HisPrcFLAG* (ABH4)	lab
ABH8-HisPrcFLAG* (ABH8)	
NSUN3-HisPrcFLAG* (NSUN3)	

*Triple (hexa)histidine (His)-preScission protease cleavage site (Prc)-FLAG octapeptide (FLAG)-tag

2.1.4 RNAs, oligonucleotides, vectors and recombinant proteins

Table 38: RNAs

Name	Sequence (5' – 3')	Purpose	Source
full-length mt-tRNA^{Met} transcript		Methylation-oxidation assay	provided by Dr. S. Haag
nt-siRNA	sense, GACAACCAACUAGUGGUGC	RNAi	Eurofins Scientific SE (Luxembourg, Luxembourg)
siABH1_1	sense, GACAACCAACUAGUGGUGC		
siABH1_3	sense, GACAACCAACUAGUGGUGC		

Table 39: Oligonucleotides

Name	Sequence (5' – 3')	Purpose	Source
ABH1_+STOP+HindIII_rev	AAAAAAAGCTTTCAGCTGTCAGGGTTTATCCTGG	Cloning (for A101)	Bohnsack lab
ABH1_oSTOP+HindIII_rev	AAAAAAAGCTTTAAGCTGTCAGGGTTTATCCTGG	Cloning (for pET28a)	

Name	Sequence (5' – 3')	Purpose	Source
ABH1_D233A_fwd	GGAATCCACGTAGCCAGATCTG AGCTAGATCACTC	Site-directed mutagenesis	Bohnsack lab
ABH1_D233A_rev	GCTCAGATCTGGCTACGTGGAT TCCCAGTGTGG		
ABH1_fwd primer	CACCATTCTGCTGTGCCCTA	qPCR	Bohnsack lab
ABH1_NcoI_fwd	AAAAAACCATGGGGAAGATGG CAGCG	Cloning	Bohnsack lab
ABH1_R338A_fwd	CTTGAAGACCGCTGCTGTTAAC ATGACTGTCCGAC	Site-directed mutagenesis	Bohnsack lab
ABH1_R338A_rev	CAGTCATGTTAACAGCAGCGGT CTTCAAGTAGCTGGC		
ABH1_rev primer	CAAGCTGCCTACCCTCAGAC	qPCR	Bohnsack lab
anti-mt-tRNA^{Met}	GGGAAGGGTATAACCAACATTT TCGGGGTATGGGCCCGATAGC TTATTTAGCTGACC	Northern blot	Bohnsack lab
GAPDH_fwd	CTGGCGTCTTCACCACCATGG	qPCR	Sigma (St. Louis, USA)
GAPDH_rev	CATCACGCCACAGTTTCCCGG		
mt-tRNA^{Met}_RT	TAATAATACAAAAAAAATATAAC CAAC	Bisulfite sequencing	Bohnsack lab
NSUN3 primer	TGGGTCTGTTTGGAATCCTATT	qPCR	Bohnsack lab
Oligo-DT primer	TTTTTTTTTTTTTTTTT	cDNA synthesis	Bohnsack lab
Tubulin primer	GCAGCCAACAACTATGCCCG	qPCR	Sigma (St. Louis, USA)

Table 40: Vectors and templates

Components	Purpose	Source
A101-ABH1 (His-MBP*-ABH1)	Cloning, site-directed mutagenesis	Bohnsack lab
pET28a-ABH1 (His-ABH1)	Cloning	Bohnsack lab
pcDNA5-ABH1-His-Prc-CFLAG	Cloning	Bohnsack lab
A1-mt-tRNA^{Met} DNA template	Bisulfite sequencing	Bohnsack lab

*Dual N-terminal (hexa)histidine (His)-maltose-binding protein (MBP) tag

Table 41: His-MBP-tagged recombinant proteins

Components	Source
His-MBP-NSUN3	Bohnsack lab, this study
His-MBP-ABH1	Bohnsack lab, this study
His-MBP-ABH1 (D233A) mutant	Bohnsack lab, this study
His-MBP-ABH1 (R338A) mutant	Bohnsack lab, this study

2.1.5 Software

Table 42: Software

Product	Company
Adobe Photoshop	Adobe, (San Jose, CA, USA)
ChemDraw	Perkin Elmer (Waltham, USA)
Lasergene	DNASTAR (Madison, WI, USA)
Mac OS X	Apple Inc. (Cupertino, CA, USA)
Microsoft Excel	Microsoft Inc. (Redmond, WA, USA)
Microsoft Word	Microsoft Inc. (Redmond, WA, USA)
Windows XP	Microsoft Inc. (Redmond, WA, USA)

2.2 Methods

2.2.1 Cell culture

2.2.1.1 Eukaryotic cell lines

HEK 293 and HeLa CCL2 cells were cultured in 10 cm^2 petri dishes in DMEM supplemented with 10 % FCS, 2 mM glutamine, 10 µg/ml penicillin and 10 µg/ml streptomycin. The cultures were grown in a humidified incubator under 5 % CO_2 at 37 °C. Medium and solutions used were sterile and warmed up to 37 °C in a water bath prior to cell treatment. Handling cells took place under a laminar flow hood. Cells were passaged regularly when cell density reaches approximately 80 – 90 % confluence. To do this, the medium was discarded, and the adherent cultures were washed with phosphate buffer. 0.25 % trypsin-EDTA was added and the dishes were incubated at 37 °C for 3 min to enable the cells to detach. Cells were re-suspended in DMEM and diluted 1:10 in fresh media and transferred to a fresh petri dish.

2.2.1.2 Prokaryotic cell lines

E. coli cells for transformation and cloning purposes were either cultivated on lysogeny broth agar plates containing the appropriate antibiotic or in liquid cultures that were incubated overnight with constant shaking at 200 – 250 rounds per minute (rpm) at 37 °C.

2.2.2 RNA interference

Knock-down of ABH1 in HEK 293 and HeLa CCL2 cells was carried out by RNA interference (RNAi) using two different small interfering RNAs (siRNAs), siRNA 1 and siRNA 3, targeting the ABH1 mRNA. A non-target siRNA was used as a control.

siRNAs were transfected using lipofectamine RNAiMax with a final concentration of 40 nM or 60 nM. Therefore, siRNAs and the transfection reagent were diluted separately with optiMEM reduced serum media and mixed. After 15 min incubation at room temperature the siRNA-lipid complex was then added to exponentially grown HeLa CCL2 cells, plated in 6 cm^2 petri dishes and incubated at 37 °C for 96 h.

2.2.3 Total RNA extraction

Total RNA was extracted from HEK 293 cells and HeLa CCL2 cells using trizol reagent according to the manufacturer's instructions. In brief, the media was removed, and cells were lysed by incubation with trizol reagent for 5 min at room temperature. Lysed cells were transferred to a sterile tube containing 200 µl of chloroform. The tubes were inverted, centrifuged for 10 min at 14000 rpm and 4 °C to pellet the cellular debris and the upper aqueous phase was transferred to fresh tube containing 500 µl of isopropanol. The tubes were left for 10 min at room temperature, and centrifuged for another 20 min at 14000 rpm and 4 °C. After washing the precipitated RNA pellet with 500 µl of 70 % EtOH (ethanol), the pellet was air-dried and suspended in 30 µl RNase-free H_2O. The isolated RNA was stored at -80 °C until use.

To monitor the quality of the extracted RNA, a 1.2 % agarose gel in 1 x BPTE buffer was poured. 2 µl of RNA sample and 10 µl glyoxal loading dye was preheated at 55 °C for 5 min and loaded onto the gel. The RNA was separated at 60 volts (V) for 2 h in BPTE buffer.

2.2.4 Complementary DNA synthesis

Total RNA was thawed on ice and the concentration was determined using a spectrophotometer. A ligation mixture containing 2 µg total RNA, 1 µl 50 µM oligo dT primer and 1 µl 10 mM dNTPs was heated at 65 °C for 5 min, stored on ice and centrifuged for 1 min at 14000 rpm.

For elongation, 4 µl first strand buffer (5 x), 1 µl 0.1 M DTT, 1 µl ribolock RNase inhibitor and 1 µl superscript III reverse transcriptase were added and the mixture was incubated at 50 °C for 1 h. Enzymes were inactivated by incubation at 70 °C for 20 min.

The products were stored at -20 °C or placed on ice for immediate use.

2.2.5 Quantitative polymerase chain reaction

SYBR green real-time polymerase chain reaction (PCR) master mix (SYBR-mix) was used according to the manufacturer’s instructions to perform quantitative PCR (qPCR). The assays were mixed including complementary DNA (cDNA) as in Table 43.

Table 43: Reaction assay of qPCR with complementary DNA

Components	Final composition
SYBR-mix	3.32 µl
Primer mix (16.6 µM)	0.2 µl
Milli-Q H_2O	3.57 µl
cDNA (1:10)	3 µl

All samples were pipetted in triplicate. The levels of the mRNAs encoding the house keeping proteins tubulin and GAPDH (glyceraldehyde 3-phosphate dehydrogenase) where monitored as controls. For quantification analysis, only triplicates with crossing point (Cp) levels that differ less than 0.5 units where used. qPCR programme was run as in Table 44.

Table 44: qPCR programme

Step	Temperature	Time	Cycles
Pre-incubation	95 °C	5 min	1
Denaturation	95 °C	10 sec	
Annealing	58 °C	20 sec	50
Elongation	72 °C	15 sec	

2.2.6 Cross-linked RNA immunoprecipitation

To determine if ABH1, ABH2, ABH3, ABH4 or ABH8 physically associate with mt-$tRNA^{Met}$, HEK 293 cell lines expressing triple (hexa)histidine (His)-preScission protease cleavage site (Prc)-FLAG octapeptide (FLAG)-tagged versions of one of these dioxygenases were used. Cell lines expressing HisPrcFLAG-tagged NSUN3 or the HisPrcFLAG tag alone were used as a positive and a negative control. All cell lines were previously created by Dr. S. Haag (see Table 39) and cross-linked RNA immunoprecipitation (IP) experiments were performed in collaboration with her.

Protein expression in cell lines was induced using 1 µg/ml tetracycline for 24 h. Every petri dish was washed twice (15 ml and 7 ml) with PBS buffer before UV-irradiation at 8000 mJ/cm^2 at 254 nm thrice using a Stratalinker 2400 UV crosslinker. All PBS was removed, 150 µl TMN 150 buffer was added to the dishes and cells were scraped, then transferred into fresh tubes. Cells were lysed by sonication (25 % intensity, 0.5 duty cycle) thrice for 15 sec with 30 sec cooling in between.

The cell lysates were centrifuged at 20000 gravitational force (g) and 4 °C for 10 min. 100 µl of the supernatant was taken as input and was subjected to PCI extraction of RNA as described in 2.2.15.1. The rest was used for pulldown experiments.

Tubes containing 100 µl of 50 % anti-FLAG M2 magnetic beads slurry were pre-equilibrated thrice with TMN 150 buffer. The cell lysates were added for a 2 h incubation at 4 °C on a rotation wheel with 50 – 70 rpm. The supernatant containing unbound proteins was removed and the beads were washed twice with 2 ml of TMN 1000 buffer and twice with 2 ml TMN 150 buffer. 600 µl of TMN 150 buffer and preScission protease was added for overnight incubation at 4 °C on a rotation wheel.

The supernatant was transferred to a tube containing preScission eluate buffer and vortexed until the guanidine HCl was dissolved. The samples were then added to the tubes containing 100 µl of nickel-nitrilotriacetic acid (Ni-NTA) slurry that has been pre-equilibrated thrice with 500 µl of Ni-NTA washing buffer I. After a 2 h binding step at 4 °C on the rotation wheel, the supernatant was removed, and the beads were washed thrice with 750 µl of Ni-NTA wash buffer I and thrice with 750 µl of Ni-NTA washing buffer II. After the washing step, beads were resuspended in 400 µl of Ni-NTA washing buffer III adding 6.5 µl of proteinase K for overnight incubation at 55 °C with shaking. The next day, the supernatant was subjected to PCI extraction of RNA as described in 2.2.15.1. 1 µl of 20 mg/ml glycogen was added to each sample before incubation at -20 °C to aid precipitation. RNA pellets were resuspended in 10 µl denaturing RNA loading dye for subsequent analysis by northern blotting.

2.2.6.1 Northern blotting of RNAs

For detection of bound tRNAs by northern blotting, RNA samples were heated at 95 °C for 5 min, and loaded onto a 12 % polyacrylamide (PAA) gel that was poured as described in Table 45,

Table 45: PAA gel mix

Components	Final concentration
Acrylamide (40 %)	30 %
TBE buffer (10 x)	10 %
Urea	7 M

The samples were separated at 120 V for 45 min in 1 x TBE buffer. RNAs were transferred on a nylon membrane in 0.5 x TBE buffer by electroblotting at 60 V for 2 h and then fixated covalently to the membrane via UV irradiation at 254 nm using a Stratalinker 2400 UV crosslinker.

To detect specific tRNAs, DNA probes were labelled radioactively with γ-[^{32}P]-ATP. Reactions containing 14.5 µl H_2O, 2 µl 10 x T4 polynucleotide kinase (PNK) buffer A, 0.5 µl 10 µM DNA oligonucleotides, 2 µl γ-[^{32}P]-ATP and 1 µl T4 PNK were incubated for 30 min at 37 °C. Membranes were incubated in pre-hybridisation buffer at 37 °C for 30 min before addition of the radiolabelled probes.

After overnight hybridization at 37 °C, the probe was removed and the membrane was washed once with SSC buffer (6 x) and with high stringency buffer at 37 °C for 30 min each, to wash off unspecifically bound probes. The air-dried blot was then exposed to a phosphoimager screen and then the radioactive signal was detected using a phosphoimager.

2.2.7 RNA bisulfite sequencing

To detect m^5C and f^5C in cellular RNAs, total RNA extracted from wild type cells and cells treated with non-target siRNAs or siRNAs targeting NSUN3 or ABH1 underwent HSO_3 (bisulfite) treatment and $NaBH_4$ (sodium borohydride) treatment followed by cDNA library preparation for analysis by NGS.

DNase digestion was performed on 6 µg of total RNA by adding turbo DNase followed by incubation for 30 min at 37 °C. RNA was re-isolated by adding 300 µl PCI, vortexing and centrifuging at 14000 rpm and 4 °C for 5 min. The upper phase was transferred to a fresh tube containing 30 µl NaAc, 1 µl 20 mg/ml glycogen and 900 µl of 100 % EtOH for overnight precipitation at -20 °C. Samples were centrifuged for 30 min at 14000 rpm and 4 °C. The supernatant was discarded, and the RNA pellet was washed with 500 µl of 70 % EtOH, followed by another 10 min centrifugation step under the same conditions. The supernatant was discarded, the pellet was air-dried for 10 min, resuspended in 21 µl RNase-free H_2O and stored at -80 °C. Half of each sample was used directly for $NaBH_4$ reduction.

2.2.7.1 $NaBH_4$ treatment

10 µl of the resuspended RNA samples were mixed with equal amounts of $NaBH_4$ solution, vortexed and the solution was incubated for 30 min on ice without light exposure. 10 µl 750 mM NaAc pH 5, 1 µl of 20 mg/ml glycogen and 100 µl of 100 % EtOH were added for overnight precipitation at -20 °C. Samples were centrifuged for 30 min at 14000 rpm and 4 °C, washed with 500 µl 70 % EtOH, centrifuged again for 10 min under the same conditions, air-dried and resuspended in 11 µl RNase-free H_2O. Then, 1 µl was taken to determine the RNA concentration using a spectrophotometer.

2.2.7.2 Bisulfite reaction

From here on, DNase digested samples and the $NaBH_4$ treated samples were treated equally. The 10 µl samples were transferred into PCR tubes, and 42.5 µl HSO_3 mix from the EpiTect bisulfite kit and 17.5 µl DNA protection buffer was added. Samples were incubated at 70 °C for 1 min and then at 60 °C for 1 h.

Samples were desalted using micro bio-spin chromatography columns according to manufacturer's instructions and further desulphonated adding 1 volume of Tris, adjusted to pH 9.0. After 30 min of incubation at 37 °C, 1/10 volume to volume 3 M NaAc pH 5, 20 µg glycogen and 3 volumes of 100 % EtOH was added for overnight precipitation at -20 °C. Samples were centrifuged for 30 min at 14000 rpm and 4 °C. The precipitation product was washed with 500 µl of 70 % EtOH, air-dried for 10 min, and resuspended in

11 µl RNase-free H_2O. Then, 1 µl was taken to determine the RNA concentration using a spectrophotometer.

RNA was prepared for NGS by first adding 5'-, and 3'-linker sequences and specifically amplify our RNA of interest, and secondly adding Illumina adapters with indices for multiplexing according to the manufacturer's protocol. The PCR fragments were isolated by agarose gel electrophoresis, subsequent gel extraction of the desired cut out bands and spin column extraction according to manufacturer's instructions.

2.2.8 Molecular cloning

Molecular cloning was carried out to generate constructs for the recombinant expression of ABH1 with dual N-terminal His-maltose-binding protein (MBP) tag (in case of A101 vector) or a C-terminal His tag (in case of pET28a) (Figure 4) in *E. coli*.

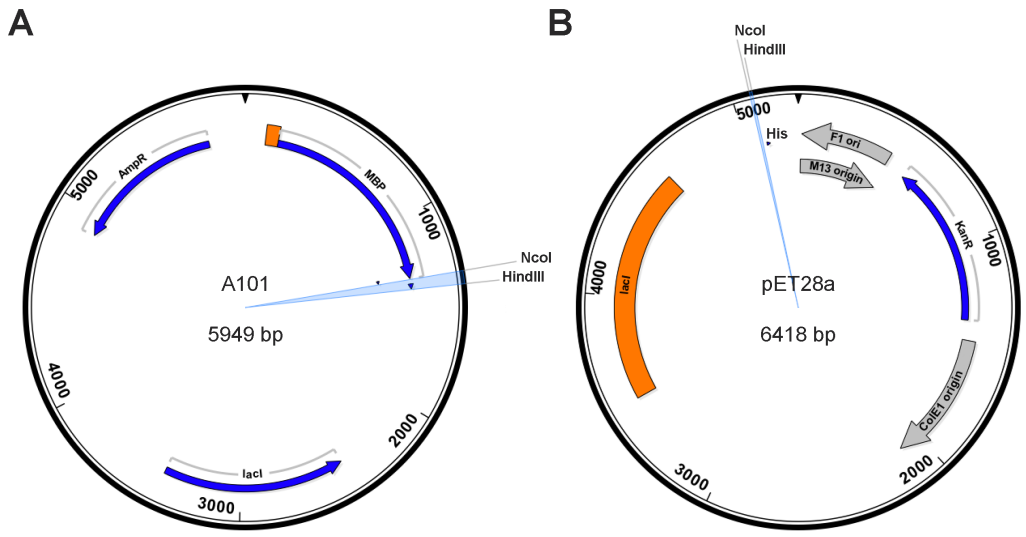

Figure 4: Maps of vectors used for molecular cloning.
Vector A101 (A) and pET28a (B) with positions of the restriction sites for cloning as indicated. Vector length in base pairs (bp).
Vector maps made in DNAStar Lasergene.

2.2.8.1 Polymerase chain reaction

The CDS of ABH1 was amplified by PCR (Mullis et al. 1992) from a pre-existing plasmid (pcDNA5-ABH1-His-Prc-CFLAG), kindly provided by Dr. S. Haag. The primers, ABH1_NcoI_fwd (for both vectors), ABH1_oSTOP+HindIII_rev (for pET28a vector) and ABH1_+STOP+HindIII_rev (for A101 vector) were

designed including restriction sites NcoI and HindIII. The assays were mixed and ran as in Table 46.

Table 46: Reaction assay of PCR for amplification of ABH1 coding sequence

Component	Final composition
dNTPs	3 µl
Milli-Q H_2O	48.5 µl
Plasmid	2 µl (33 ng/µl)
Primer I	2 µl
Primer II	2 µl
Taq polymerase (10 x)	1.5 µl
Taq polymerase buffer	5 µl

Amplification reaction was performed using a thermal cycler under the following conditions as in Table 47.

Table 47: Programme of PCR for amplification of ABH1 coding sequence

Step	Temperature	Time	Cycles
Pre-incubation	95 °C	5 min	1
Denaturation	95 °C	30 sec	
Annealing	58 °C	30 sec	50
Elongation	72 °C	1 kb/min	
Final elongation	72 °C	5 min	1

Correct product length was visualised on a 1 % agarose gel, run in 1 x TAE buffer, relative to a DNA marker. The generated PCR products were purified using the nucleospin gel and PCR clean-up kit according to the manufacturer's instructions.

2.2.8.2 Restriction digestion

To create compatible cohesive ends, both the purified PCR products (1.1 µg/µl) and the target vectors A101 (14 ng/µl) and pET28a (31 ng/ml) underwent a 2 h restriction digest at 37 °C by the recipe in Table 48.

Table 48: Restriction digest of purified ABH1 amplicon or target vectors

Component	Final composition
HindIII	2 µl
NcoI	2 µl
PCR product or target vectors	1 or 10 µl
Tango buffer	20 µl
Milli-Q H_2O	ad 40 µl

Target vectors A101 and pET28a underwent subsequent 10 min dephosphorylation using fastAP thermosensitive alkaline phosphatase after restriction digest. Two times 10 µl of each digestion product was mixed with 2 µl of DNA gel loading dye (6 x), separated on a 1 % agarose gel in 1 x TAE buffer containing safeview nucleic acid stain, and bands that represent the cleaved vectors or PCR products were cut out and purified using nucleospin gel and PCR clean-up kit.

2.2.8.3 Ligation

Once the inserts and the target vectors were digested and purified, ligation was performed for 60 min at 37 °C as in Table 49.

Table 49: Ligation reaction of ABH1 insert and target vectors

Component	Final concentration
ABH1 insert	3 µl (50 ng/µl)
Ligase buffer (10 x)	2 µl
T4 DNA ligase	1 µl
Target vector (A101 or pET28a)	1 µl (50 ng/µl)
Milli-Q H_2O	ad 20 µl

Ligation reaction containing just the cut vector and no insert was used for further steps as negative control.

2.2.8.4 *E. coli* transformation

The ligation reaction was used to transform 75 µl of one shot TOP10 chemically competent *E. coli* cells. The transformation mix was incubated on ice for 20 min, heat shocked at 42 °C for exactly 90 sec and cooled down for 1 min on ice. After adding 1 ml of S.O.C. media, cells were incubated for 40 min at 37 °C before a 3 min centrifugation step at 1700 x g. The supernatant was decanted, pelleted cells were re-suspended in remaining media and plated onto lysogeny broth amp-agar plates in case of A101 vector, and lysogeny broth kan-agar plates in case of pET28a vector. Plates were incubated overnight at 37 °C.

2.2.8.5 Identification and sequencing of positive clones

Five individual colonies of each plate were picked randomly and used to inoculate in 5 ml lysogeny broth kan/lysogeny broth amp media, which was grown overnight at 37 °C with shaking.

Cultures were diluted 1:50, incubated at 37 °C to reach optical density at a wavelength of 600 nm (OD_{600}) of 0.6, centrifuged for 30 sec at 20000 x g, and the supernatant was discarded. For isolation of plasmids, the nucleospin plasmid kit was used according to the manufacturer's instructions.

In order to identify positive clones, 1 µl of purified plasmid was used for analytical restriction digest with restriction enzymes NcoI and HindIII as previously described in 2.2.8.2. The products were separated on 1 % agarose gel in TBE buffer and positives clones were identified based on the excision of a fragment of the correct size. 5 µl (approximately 80 ng/µl) was sent for Sanger sequencing at GATC Biotech Cologne to confirm the insert sequence.

2.2.9 Site-directed mutagenesis

The production of two catalytically inactive ABH1 mutants, D233A and R338A, by site-directed mutagenesis, was carried out using the A101 vector (ABH1 with

N-terminal His-MBP tag). Reaction assays were composed as in Table 50 following the PCR programme in Table 51.

Table 50: Reaction assay of PCR for amplification of ABH1 mutants

Component	Final composition
dNTPs (2.5 mM)	5 µl
Phusion HF buffer pack	10 µl
Phusion HF DNA polymerase	0.5 µl
Primer mix (10 µM)	2 µl
Template plasmid	2 µl (22 ng/µl)
Milli-Q H_2O	ad 50 µl

Table 51: Programme of PCR for amplification of ABH1 mutants

Step	Temperature	Time	Cycles
Pre-incubation	95 °C	5 min	1
Denaturation	95 °C	30 sec	
Annealing	62 °C	30 sec	30
Elongation	72 °C	15 min	
Final elongation	62 °C	20 min	1

The four oligonucleotides, ABH1_D233A_fwd, ABH1_D233A_rev, ABH1_R338A_fwd and ABH1_R338A_rev, that were used as primers contain a point-mutation designed to induce the desired amino acid substitution in the expressed protein and were complementary each other and to the mutation site (see Figure 7). The amplification products were treated with 1 µl DpnI restriction enzyme at 37 °C for 2 h to degrade the methylated DNA template.

The digestion products were PCI and EtOH precipitated as described in 2.2.15.1. The DNA was used to transform 75 µl of one shot TOP10 competent cells as described in 2.2.8.4. Plasmid DNA was extracted from single colonies as described in 2.2.8.5 and correctly mutated plasmids were identified by Sanger sequencing at GATC Biotech.

2.2.10 Protein expression

For recombinant expression of His-MBP-ABH1 and the two mutants (D233A and R338A) in *E. coli*, the appropriate constructs used to transform 50 µl of rosetta DE3 pLysS competent (rosetta) cells following the same protocol as described in 2.2.8.4. 20 ml of lysogeny broth amp-can media pre-cultures were inoculated and grown overnight under vigorous shaking. The overnight cultures were diluted 1:50 in 500 ml lysogeny broth amp-can media and grown at 37 °C until the OD_{600} reached 0.6 when expression was induced by adding 0.5 mM IPTG, followed by overnight incubation at 18 °C. 1 ml samples were taken before and immediately after induction as non-induced and induced controls. Cells were harvested by centrifugation for 20 min at 6000 rpm, washed with PBS, transferred into 50 ml tubes, snap frozen in nitric oxide and stored at -20 °C.

2.2.11 Protein purification

Protein purification by immobilised-metal affinity chromatography (IMAC) took place in a cold room at 4 °C and involved the use of complete His-tag purification resin to retrieve proteins via their His tags. Samples were taken after each step and stored at -20 °C for later SDS-polyacrylamide gel electrophoresis (PAGE) analysis. First, cell pellets were resuspended in 20 ml sonication buffer containing one tablet of complete mini protease inhibitor cocktail and sonicated as described in 2.2.6. Total lysates were centrifuged at 20000 x g for 15 min at 4 °C to pellet the cellular debris. Chromatography columns were filled with 0.5 ml of 50 % Ni-NTA slurry and washed with 5 ml of sonication buffer for equilibration, allowing the solution to flow out. The cleared lysates were added to the columns for a 30 min incubation on a rotation wheel.

The beads were washed with 10 ml of sonication buffer for two cycles, followed by 15 min incubation with 5 ml of IMAC washing buffer for three cycles. Washed beads were rinsed with 0.5 ml of IMAC elution buffer followed by another 10 min incubation in the buffer. The eluates were pooled and transferred to dry spectra regenerated cellulose membrane dialysis sacks and incubated in 1000 ml of dialysis buffer I for 3 h and in 1000 ml of dialysis buffer II overnight. Dialysed protein was transferred from the membrane to fresh tubes and stored at -20 °C.

2.2.12 Determining protein concentration

For the measurement of the protein concentration, a colorimetric protein assay after the Bradford method (Bradford 1976) was used. It is based on a shift in the absorbance maximum detected by a spectrophotometer when coomassie dye associates with proteins. 990 µl of bradford reagent was mixed with 2 µl of the dialysed sample and 8 µl of milli-Q H_2O and incubated for 10 min at room temperature in the dark before determining the absorbance at 595 nm. One sample containing dialysis buffer I instead of the dialysed protein was used as blank value.

A calibration curve with bovine IgG dilutions of known concentrations was made beforehand and the protein concentrations of the wild type ABH1 and mutant samples was then determined by interpolation.

2.2.13 Sodium dodecyl sulfate-polyacrylamide gel electrophoresis analysis

The samples taken during purification of recombinant ABH1 and its mutants were analysed by SDS-PAGE (Laemmli 1970). 10 µl of SDS-PAGE loading dye was added to each sample and they were denatured at 95 °C for 10 min, then stored on ice. For separation of the proteins, 12 % gels were poured as described in Table 52, samples were loaded and separated at 25 mA per gel for 2 – 4 h in laemmli buffer.

Table 52: Components for SDS-PAGE (sufficient for two 12 % gels)

Component	Resolving gel	Stacking gel
Acrylamide (30 %)	4.2 ml	0.8 ml
APS	100 µl	100 µl
Milli-Q H_2O	3.3 ml	2.9 ml
TEMED	20 µl	20 µl
Tris (1.5 M, adjust to pH 8.0)	2.5 ml	–
Tris (0.55 M, adjust to pH 6.8)	–	1.25 ml

To visualize the separated proteins, the gels were incubated in boiled milli-Q H_2O for 10 min first to wash out the SDS, then stained with colloidal coomassie

staining solution overnight. The gels were washed with milli-Q H_2O and scanned.

2.2.14 *in vitro* transcription

For the *in vitro* methylation and oxidation experiments, mt-tRNA^{Met} was *in vitro* transcribed from a pre-existing A1-mt-tRNA^{Met} DNA template including a T7 promotor and the mt-tRNA^{Met} sequence, made available by Dr. S. Haag. For each *in vitro* transcription, three reactions were run in parallel and pooled after gel purification.

The template was added to the reaction mixture (Table 53), that was incubated for 1 h at 37 °C, before a 15 min DNA digestion by addition of 1 µl of turbo DNase.

Table 53: *in vitro* transcription

Component	Final composition
A1-mt-tRNA^{Met}	500 ng
NTPs (5 mM)	10 µl
Ribolock RNase inhibitor	1 µl
RNase-free H_2O	ad 50 µl
T7 RNA polymerase	2 µl
Transcription buffer (5 x)	10 µl

Transcription products were purified by gel filtration chromatography using mini quick spin RNA columns that were prepared according to the manufacturer's instructions prior use. The products were applied to the columns that were centrifuged at 1000 g for 4 min. The eluates were transferred into fresh tubes and stored at -80 °C until use. Correct transcript size was checked by comparing with pre-existing mt-tRNA^{Met} via denaturing urea PAGE as described in 2.2.15.4.

2.2.15 *in vitro* methylation-oxidation assay

The methylation and oxidation experiments took place in an isotope lab. To avoid contamination when working with radioactive ^3H (tritium), gloves were

changed regularly, wipe tests were performed after each experiment, and tubes were centrifuged shortly after each step. ^{3}H-, and phenol contaminated tubes and vials where disposed of in designated waste.

2.2.15.1 Methylation assay

Recombinant NSUN3 for methylation of the mt-tRNA^{Met} *in vitro* transcript was kindly provided by Dr. S. Haag. For each oxidation reaction, one 20 µl ^{3}H-methylation assay and one more sample (n+1) was prepared. The following components were mixed in the listed order as in Table 54.

Table 54: Methylation assay

Component	Final composition
^{3}H-SAM	2 µl
NSUN3	3 µl (1 µg/µl)
Methylation buffer (10 x)	2 µl
mt-tRNA^{Met}	2.1 µl (260 µg/µl)
Ribolock RNase inhibitor	1 µl
Milli-Q H_2O	ad 20 µl

The methylation assay was pre-incubated for 5 min at 22 °C without the mt-tRNA^{Met}, and subsequently incubated for 2 h at 22 °C. The reaction was stopped by adding 1 µl of proteinase K and incubated for another 30 min at 22 °C. The samples were pooled, 3 M NaAc (pH 5.2) and PCI in 1:1 ratio was added and mixed carefully until milky. After a 5 min centrifugation step at 20000 x g, the upper aqueous phase was transferred into a fresh tube, and 100 % EtOH in 1:1 ratio was added. The samples were stored at -20 °C overnight. The samples were centrifuged for 30 min at 20000 x g and 4 °C, then the supernatant was discarded. After washing the precipitated RNA with 500 µl of 70 % EtOH, the pellet was air-dried for 10 min and resuspended in 4 µl milli-Q H_2O per assay.

2.2.15.2 Oxidation assay

For oxidation of ^{3}H-methylated mt-tRNA^{Met} the purified His-MBP-ABH1 and the two mutants (D233A and R338A) were used. The following components were mixed in the listed order as seen in Table 55.

Table 55: Oxidation assay

Component	Final concentration
^{3}H- mt-tRNA^{Met}	3 µl
ABH1, FTO*, MBP or no enzyme**	3 µl (1 µg/µl)
Fe^{2+}**	2 µl (50 µM/µl)
Oxidation buffer	2 µl
Ribolock RNase inhibitor	1 µl
α-Ketoglutarate*	2 µl (50 µM/µl)
Milli-Q H_2O	ad 20 µl

* In case of FTO, due to concentration 4 µl was added.

** In assays with no enzyme, no α-ketoglutarate, or no Fe^{2+}, volume was compensated with Milli-Q H_2O.

The oxidation assay was incubated for 1 h at 22 °C. 1 µl of proteinase K was added, and incubated for another 30 min at 22 °C. 80 µl of milli-Q H_2O, 10 µl of 3 M NaAc (pH 5.2), 1 µl of glycogen (20 mg/ml) and 300 µl of 100 % EtOH was added to each sample, and the product was stored for 2 h at -20 °C.

2.2.15.3 Scintillation counting

Samples were centrifuged for 30 min at 20000 x g and 4 °C. The supernatant was then transferred to scintillation vials with 2 ml lumasafe plus scintillation liquid. The pellet was washed with 500 µl of 70 % EtOH, air-dried and resuspended in 10 µl milli-Q H_2O. 1 µl of each sample was transferred to vials containing 2 ml scintillation liquid. 10 µl of denaturing RNA loading dye was added to the remaining sample and stored at -20 °C for later gel analysis. Scintillation vials with 300 µl of 100 % EtOH or 1 µl of milli-Q H_2O were used as negative controls. All vials were inverted five times, stored for 3 min and transferred to the scintillation counter.

2.2.15.4 Analysis of *in vitro* methylation samples

The samples of the resuspended pellets generated after the methylation and oxidation experiments were separated via denaturing urea-PAGE (Table 56). Probes were preheated at 55 °C for 5 min and the gel underwent pre-run for 30 min. Wells were rinsed twice with a syringe to ensure proper loading. The gel ran in TBE buffer at 500 V and 30 mA for 2 h.

Table 56: Components of 12 % denatured urea PAGE

Component	Final composition
Acrylamide (40 %)	15 ml
APS (20 %)	100 µl
MOPS buffer	1 µl
TBE (5 x)	10 ml
TEMED	100 µl
RNAse-free H_2O	10 ml
Urea (7 M)	21 g

The gel was stained with ethidium bromide for detection of the transcripts followed by incubation for 15 min in 250 ml of fixing solution for two times before a 45 – 60 min incubation step in genamp100 amplify fluorographic reagent. A Whatman paper was placed on a gel dryer, the gel was placed on top carefully to avoid air bubbles in between and covered with a gel drying film. The gel was dried at 65 °C for 2 h under vacuum pressure. After drying, the gel was exposed to an x-ray film for 14 h at -80 °C, and the radioactive signal was detected by developing.

3 Results

3.1 Background

Mapping and characterisation of RNA modifications and the identification of their modifying enzymes describe one focus of research in the Bohnsack lab. These modifications are involved in all aspects of gene expression and their link to human diseases attracts growing attention.

One target of RNA modifying enzymes is the pyrimide base C34 of mt-tRNA^{Met}. Preliminary data of the Bohnsack lab identified C34 of mt-tRNA^{Met} as substrate of NSUN3, one so far uncharacterised putative methyltransferase, that has been subject of investigation. *In vitro* assays could show that C34, which is located at the wobble position of the tRNAs anticodon stem-loop, is a target nucleotide of NSUN3 (Haag et al. 2016). Interestingly, previous reports suggested a formylation instead of methylation of C34, raising the question which enzyme might be responsible for converting m^{5}C34 into f^{5}C34 as part of a dynamically step-by-step-like modification of the RNA.

Likely candidates for the conversion of C34 include the AlkB dioxygenase family of proteins ABH1 – 8 and FTO, for which nine homologs exist in humans, that can catalyse this type of chemical reaction. ABH1, a specific type of dioxygenase and part of the AlkB family has been shown to be localised in mitochondria, which made it a likely candidate for the conversion of m^{5}C to f^{5}C.

3.2 Interaction of ABH1 and mt-tRNA^{Met}

In the beginning, to determine if ABH1 directly interacts with mt-tRNA^{Met}, the aim was to perform RNA-IP experiments after UV crosslinking followed by northern blotting to detect direct protein-RNA interactions. For this reason, previously generated stably transfected HEK 293 cell lines expressing either C-terminally HisPrcFLAG-tagged NSUN3 or ABH1, or just a FLAG tag were UV-irradiated at 254 nm to create irreversibly linked protein-RNA complexes.

After tandem affinity purification on anti-FLAG and nickel (Ni^{2x}) matrices under native and denaturing conditions, the enriched complexes were eluted, and the

proteins were digested. RNA was isolated and separated by denaturing PAGE, transferred onto a nylon membrane followed by northern blot analysis using probes against the mt-tRNAs of interest.

Interestingly, mt-tRNA^{Met} was present in the eluates of FLAG-tagged ABH1 as well as the NSUN3-derived samples but not present in the eluate of the FLAG-tag control sample. This indicates that mt-tRNA^{Met} does indeed associate directly with ABH1 as well as NSUN3 (Figure 5).

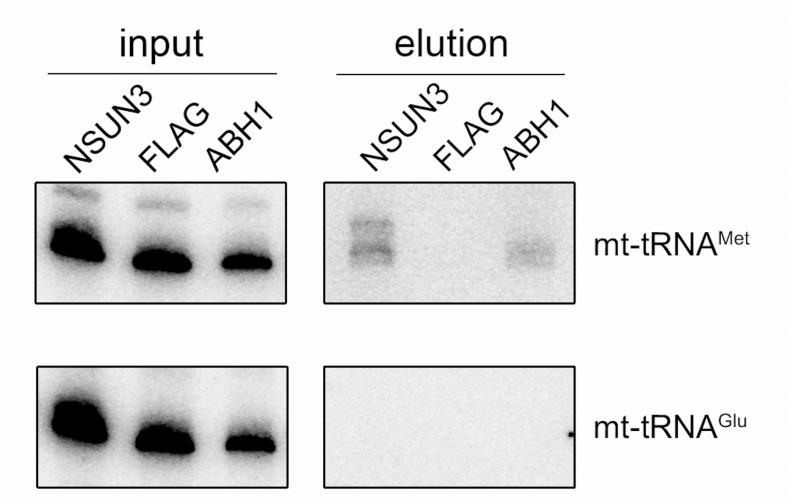

Figure 5: mt-tRNA^{Met} is specifically associated with NSUN3 and ABH1.
HEK 293 cells overexpressing FLAG-tagged versions of NSUN3 or ABH1 or the FLAG-tag alone were used for RNA immunoprecipitation (RNA-IP) experiments after UV crosslinking. RNA from inputs and eluates were separated by denaturing polyacrylamide (PAA) gel electrophoresis followed by northern blotting for mt-tRNAMet or mt-tRNAGlu.

In order to exclude that NSUN3 and ABH1 non-specifically associate with mt-tRNAs, another probe against mt-tRNA^{Glu} was used to probe the membrane. Although this tRNA was detected in the input samples, no signal was detected in the elution fractions, emphasising the specific interaction between NSUN3/ABH1 and mt-tRNA^{Met}.

3.3 *in vitro* oxidation of m^{5}C34 of mt-tRNA^{Met} by ABH1

These findings suggested that ABH1 might indeed mediate oxidation of m^{5}C34 of mt-tRNA^{Met} to f^{5}C. To test this, *in vitro* assays were established to monitor oxidation of m^{5}C34 of mt-tRNA^{Met} by ABH1.

The first step was to prepare plasmids for recombinant expression of wild type ABH1 and catalytically inactive mutants in *E. coli*. For this reason, the CDS of

the human protein ABH1 was amplified from a pre-existing vector template (Figure 6 A) by PCR. The purified PCR products and the target plasmids (A101 for expression of N-terminally His-MBP-tagged proteins and pET28a for expression of C-terminally His-tagged proteins) were restriction digested. The appropriate bands were excised, and the DNA extracted. Then the PCR products were cloned into the target vectors. Plasmids derived from five individual colonies of each transformation were checked by analytical restriction digestion (Figure 6 B). DNA fragments corresponding to the size of the ABH1 CDS insert (approximately 1170 bp) were excised in all cases suggesting successful ligation. The identity of clones A101 1 and 3 and pET28a 3 and 5 were confirmed by Sanger sequencing at GATC Biotech before proceeding.

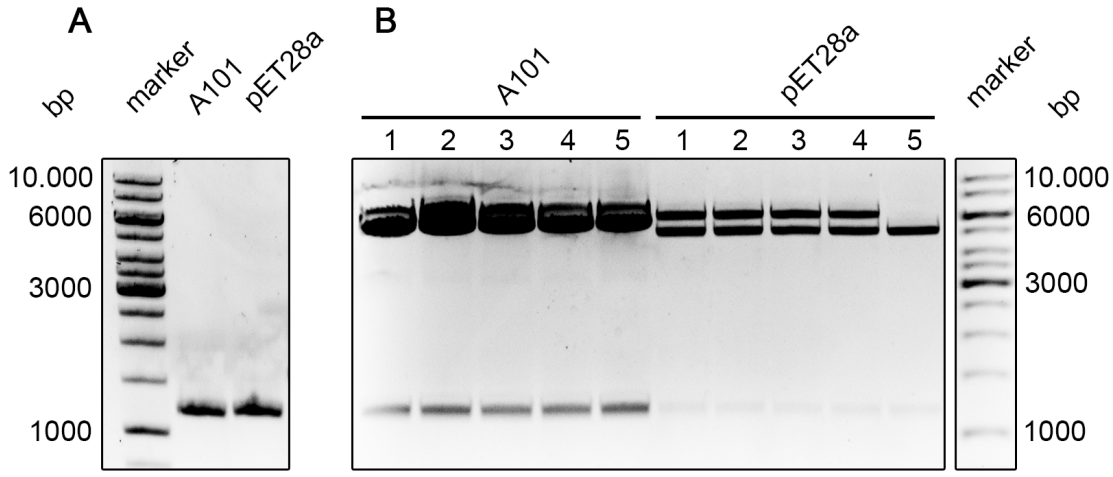

Figure 6: Cloning of ABH1 for recombinant protein expression.
A The coding sequence (CDS), approximately 1170 base pairs (bp), was amplified by PCR using two alternative primer pairs containing restriction sites for cloning into A101 and pET28a vectors as indicated. Products were visualised on a 1 % agarose gel relative to a DNA marker. **B** Candidate plasmids from the A101 (1 – 5) and pET28a (1 – 5) cloning were extracted and restriction digested to release successfully cloned inserts, representing the excised ABH1 CDS. Fragments of approximately 5000 bp represent the vectors.

Successfully generated plasmids were used to transform *E. coli* cells for subsequent protein expression and purification. To prove that any activity observed for ABH1 in the *in vitro* assays is specific for ABH1, it was also necessary to be able to express catalytically inactive ABH1 mutants. I therefore applied the method of site-directed mutagenesis, targeted to change aspartic acid (Asp or D) on position 233 to alanine (Ala or A) (D233A) and arginine (Arg or R) on position 338 to alanine (R338A) of the *ABH1* gene (Westbye et al. 2008; Bleijlevens et al. 2012). These two specific amino acids act as binding

sites for α-ketoglutarate and iron (Fe^{2+}), two cofactors of ABH1 that are necessary for proper enzyme activity (Figure 7).

In this method, primers were designed that are complementary to the mutation site, followed by PCR and digestion of the original template DNA (A101-ABH1). Products where used to transform competent *E. coli* cells, cultures were grown, plasmids extracted, and possible candidates were sent to DNA sequencing. The sequencing results showed successful preparation of plasmids for expression of mutant ABH1 (Figure 7 B and C).

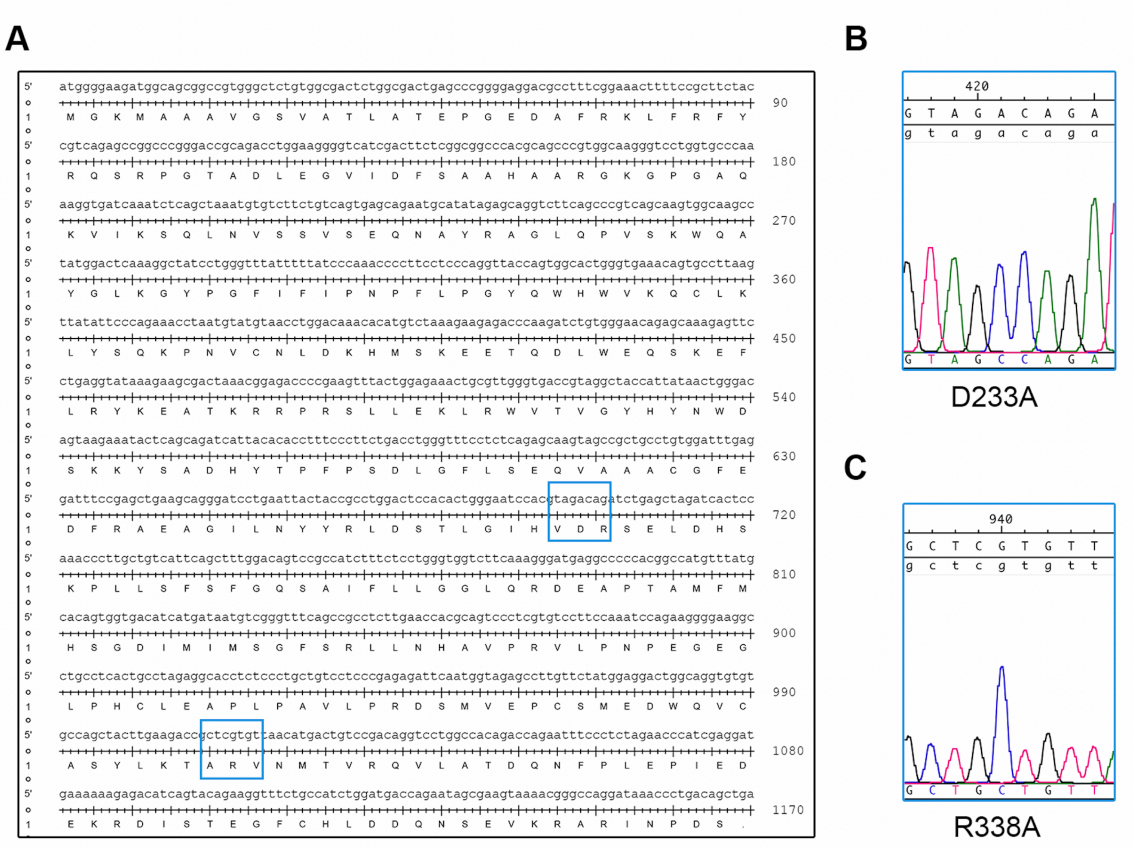

Figure 7: Coding sequence of ABH1 with mutation sites and sequencing results.
A The complete coding sequence (CDS) of ABH1, 1170 base pairs (bp), is shown on the nucleotide (upper) and amino acid (lower) levels. Indicated by the two blue boxes are the two amino acid sequences targeted for mutation.
B and C Electropherogram results of the sequence of the newly synthesised plasmids for expression of $ABH1^{D233A}$ (GAC → GCC) and $ABH1^{R338A}$ (CGT → GCT).

Having prepared the plasmids for expression of His-MBP tagged ABH1, $ABH1^{D233A}$ and $ABH1^{R338A}$, the next step was to express and purify these proteins of interest. To this end, the plasmids were used to transform in *E. coli* rosetta cells. Cultures were grown and protein expression was induced upon

addition of IPTG. Cells were lysed and the cleared lysate was incubated with nickel beads to bind their N-terminal His-MBP tag.

Analyses of samples harvested throughout the protein purification protocol by SDS-PAGE and coomassie staining showed that after induction by IPTG, ABH1 was significantly overexpressed (Figure 8 A). Some protein was insoluble (pellet) whereas some was soluble and found in the flow-through, which can be explained by high concentration of expressed proteins. After binding to nickel beads, predominantly nothing was lost during the washing steps. After elution with elution buffer, the desired protein was present and enriched (Figure 8 A).

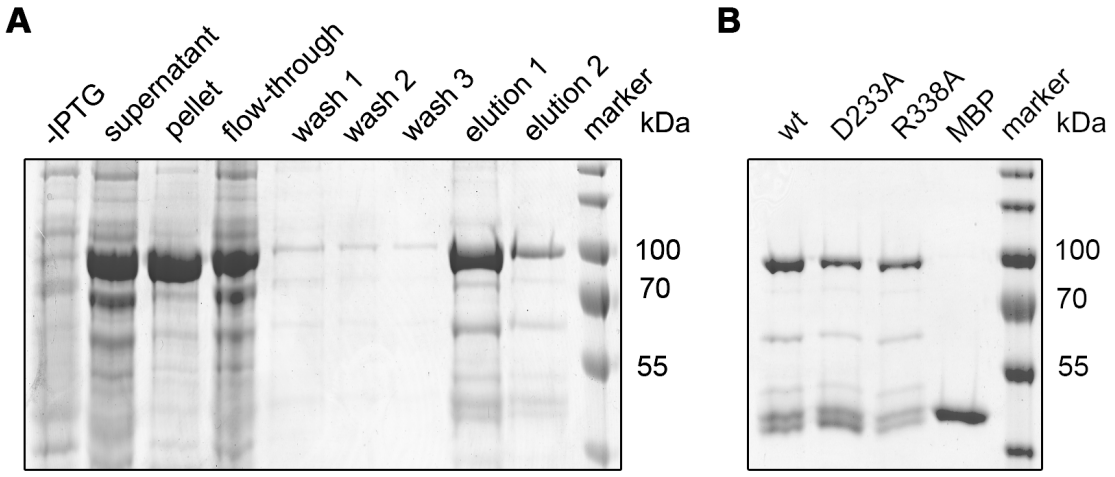

Figure 8: Expression and purification of recombinant ABH1 and mutants from *Escherichia coli*.

A Coomassie stained gel after sodium dodecyl sulfate (SDS)-polyacrylamide gel electrophoresis (PAGE) analysis of samples taken during protein expression and purification. Samples before induction (-IPTG), samples of the supernatant and pellet after sonication, material not bound to the beads (flow-through) and samples of each of the washing steps (wash 1 – 3) and elution steps (elution 1 – 2) were analysed. Product sizes given in kilodaltons (kDa).

B Coomassie stained gel after SDS-PAGE analysis of purified His-MBP tagged ABH1 (approximately 90 kDa) wild type (wt), ABH1 mutants (D233A and R338A) and the MBP tag alone (approximately 42 kDa) as control.

The mutants were similarly expressed and purified and yielded protein preparations of similar quality (Figure 8 B). In addition, the MBP tag alone was purified to use as control in the *in vitro* methylation/oxidation assay.

Having prepared recombinant proteins, the next step was to perform the *in vitro* oxidation assay. Unmodified C34 of a chemically synthesised full-length mt-tRNA^{Met} transcript kindly provided by Dr. S. Haag had to be methylated first,

which was accomplished by methylation reaction containing recombinant methyltransferase NSUN3 and ^{3}H-labelled SAM as ^{3}H-donor (Figure 9, first chemical reaction).

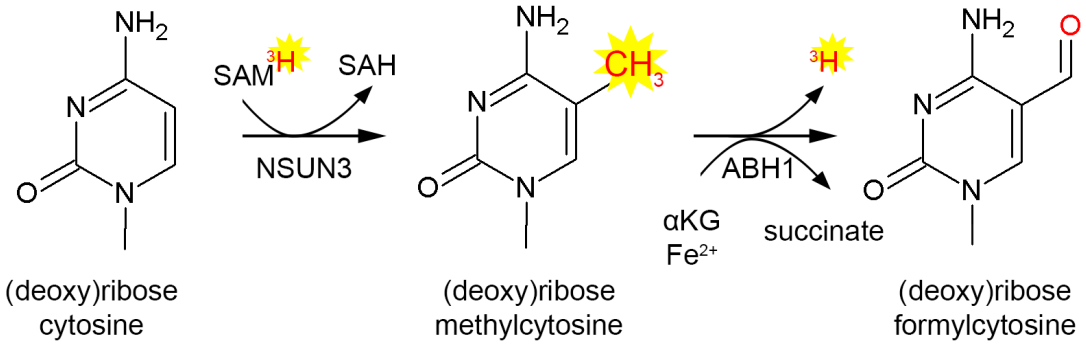

Figure 9: Reaction scheme of methylation and oxidation of C34 in mt-tRNA^{Met}.
Schematic view of *in vitro* methylation (first chemical reaction) and oxidation (second chemical reaction) of the (deoxy)ribose cytosine by methyltransferase NSUN3 and dioxygenase ABH1 showing the chemical structures of the intermediates. Abbreviations: Fe^{2+} – Iron (II) sulfate, SAH – S-Adenosyl homocysteine, SAM – S-Adenosyl methionine, αKG – α-Ketoglutarate, ^{3}H – Tritium.

Radioactively labelled m^{5}C34-mt-tRNA^{Met} was then incubated either with wild type ABH1 or two catalytically inactive mutants (ABH1^{D233A}, ABH1^{R338A}). Oxidation reactions lacking the important cofactors (α-ketoglutarate and Fe^{2+}) were included as controls. Setups containing no enzyme, MBP or FTO, another well-characterised dioxygenase, were included as additional controls. Oxidation was monitored using scintillation counting to measure the release of ^{3}H during the oxidation reaction (Figure 9, second chemical reaction). While no oxidation was observed in the absence of ABH1 or when MBP was present, wild type ABH1 efficiently oxidised m^{5}C34, indicated by a significant release of ^{3}H (Figure 10 A). To further validate this outcome, I analysed the transcripts used as substrates in the assay by denaturing PAGE. Ethidium bromide staining of the gel showed that the same amounts of transcript were present in each reaction, indicating that the differences in the quantity of ^{3}H detected were due to different levels of oxidation (Figure 10 B).

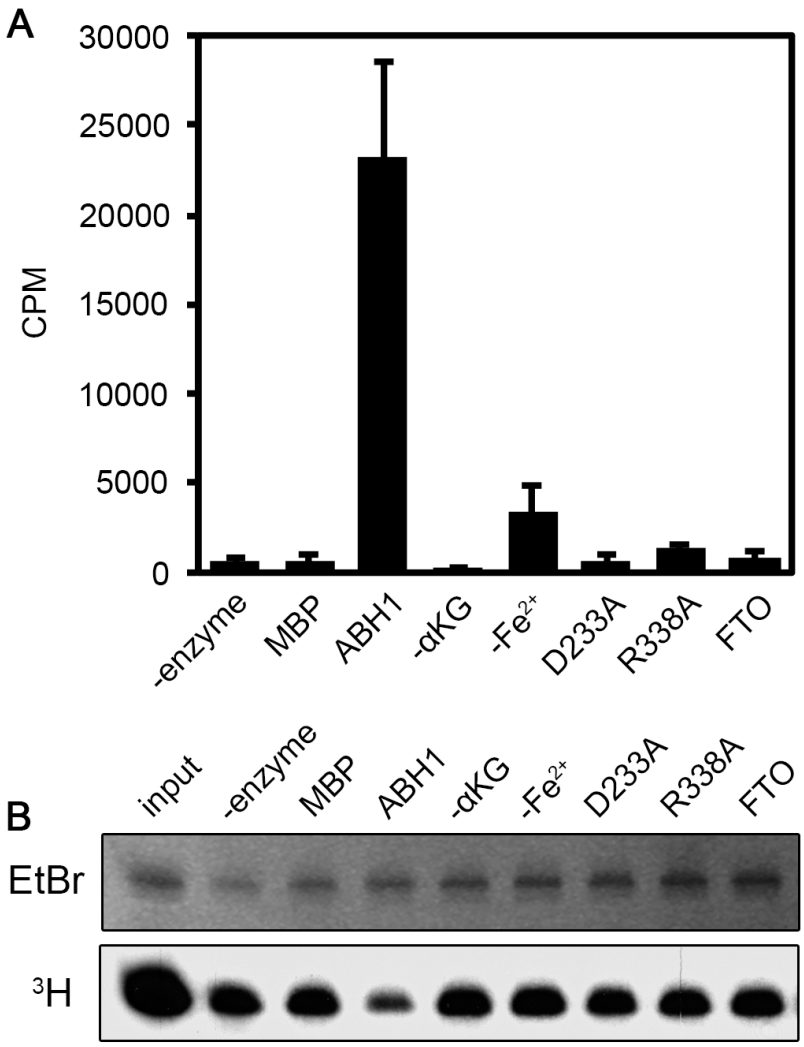

Figure 10: Oxidation of m^{5}C34 of mt-tRNA^{Met} by ABH1 *in vitro*.
A Three independent *in vitro* oxidation experiments of the full-length mt-tRNA^{Met} were measured by scintillation counting, comparing oxidation by wild type ABH1 (ABH1) to seven controls. Oxidation reaction in absence of the enzyme (-enzyme), in presence of His-MBP tag (MBP), in absence of α-ketoglutarate (-αKG) or Iron (-Fe^{2+}) and in presence of the two ABH1 mutants (D233A and R338A) and another dioxygenase (FTO).
B Transcripts after the oxidation reaction were separated on a denaturing polyacrylamide (PAA) gel. Staining with ethidium bromide (EtBr) shows the amount of transcript present in each reaction. Tritium (^{3}H) in the samples was detected by signal amplification, gel drying and exposure to an x-ray film.

As transcripts were radioactively labelled, the amount of ^{3}H left on the RNA after the oxidation reaction was also monitored using autoradiography (Figure 10 B). Exposure to an x-ray film showed that the amount of m^{5}C34 left was reduced in the sample containing ABH1 but not the mutant versions, MBP, FTO or the reactions lacking α-ketoglutarate or Fe^{2+}, which is consistent with

efficient and specific oxidation by ABH1. These results imply that ABH1 can oxidise m^5C34 to f^5C34 *in vitro*.

3.3.1 ABH1 can be efficiently depleted by RNA interference

To confirm the role of ABH1 generating f^5C34 in mt-$tRNA^{Met}$ *in vivo*, it was necessary to deplete the protein from human cells. Hence, RNAi against ABH1 was established. In this widely used method synthetic siRNAs are transfected into cells, bind and inactivate specific mRNAs to downregulate endogenous protein levels. Two different siRNAs targeted against ABH1 were tested at two different concentrations. siRNAs were transfected into HeLa CCL2 cells and after 96 hours, cells were harvested, and RNA was extracted. To check RNA integrity, the extracted RNA was analysed by denaturing agarose gel electrophoresis. The total RNA was separated on a denaturing agarose gel that was thereafter stained with ethidium bromide (Figure 11 A). The images taken with exposure to UV light revealed that the long and highly abundant 28S and 18S ribosomal RNAs were intact proofing a good quality of the obtained RNA.

To determine the level of ABH1 mRNA in cells depleted or not depleted of ABH1, qPCR analyses was used. The RNA was first reverse transcribed from an oligo-dT (a short sequence of deoxy-thymidine nucleotides) primer that anneals to the poly(A) (a short sequence of adenosine monophosphates) tail present on mature mRNAs. qPCR reactions were performed with primers that specifically amplify a region of the ABH1 mRNA. For normalisation and relative quantification, primers detecting GAPDH and tubulin mRNAs, two proteins that are stably expressed in many different cell types, were used.

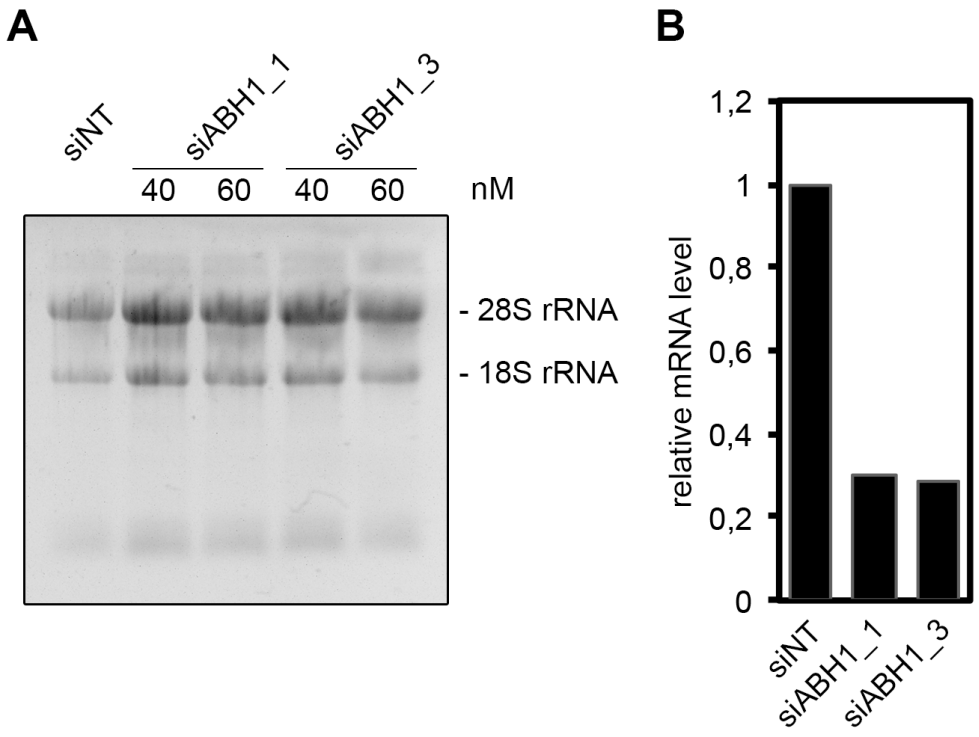

Figure 11: Depletion of ABH1 by RNA interference.
A BPTE gel showing separated RNA of two different ABH1 siRNAs (siABH1_1 and siABH1_3) of two different concentrations (40 and 60 nM) and non-target siRNA (siNT). The two main fragments in each lane represent stable 28S and 18S rRNA.
B Relative mRNA levels of ABH1 after siRNA treatment (40 nM and 60 nM pooled, 96 h) by two different siRNAs. ABH1 knock-down samples were measured in two independent experiments by quantitative polymerase chain reaction (qPCR) using GAPDH and tubulin as references and normalised to cells treated with non-target siRNA.

Normalisation of the ABH1 mRNA level according to the mean of the GAPDH and tubulin-levels showed that the amount of ABH1 mRNA was reduced approximately five-fold in cells treated with siRNA1 or siRNA3 compared to non-target siRNA (Figure 11 B). This result confirmed a method by which ABH1 could be efficiently depleted from HeLa CCL2 cells.

3.4 Analysis of the role of ABH1 in forming f^5C34 in mt-$tRNA^{Met}$ *in vivo*

Next, I wanted to analyse the levels of f^5C34 in mt-$tRNA^{Met}$ *in vivo* and see if they are dependent on the level of ABH1. The approach used to test an altered modification pattern in the presence and absence of ABH1 was RNA bisulfite sequencing (BS): bisulfite treatment (BT) or reduced bisulfite treatment (RBT) followed by Sanger sequencing. The method of BS relies on the selective

deamination of cytosine to thymine (C → T) by treatment with HSO_3 in neutral and acidic solutions. Compared to unmodified cytosine, m^5C shows only very low reactivity with HSO_3 under these conditions preventing conversion to uracil (thymine in the final readout) ($m^5C \rightarrow C$), and f^5C behaves as unmodified cytosine converting relatively efficiently to uracil/thymine ($f^5C \rightarrow T$; Figure 12, left panel). Conversion of the treated RNA to a cDNA library followed by sequencing thus allows us to distinguish between methylated and unmodified bases, but not between formylated and unmodified bases. In order to differentiate between formylated and unmethylated cytosine, RBT can be used. Half of each sample was therefore treated with $NaBH_4$ first, reducing formylated bases to 5-hydroxymethylated-m^5C (hm^5C) (Figure 12, right panel), which mimics an m^5C upon bisulfite treatment ($hm^5C \rightarrow C$).

Comparing sequencing data obtained from untreated samples, samples after BT or RBT, allowed differentiation between m^5C, f^5C and unmodified cytosine.

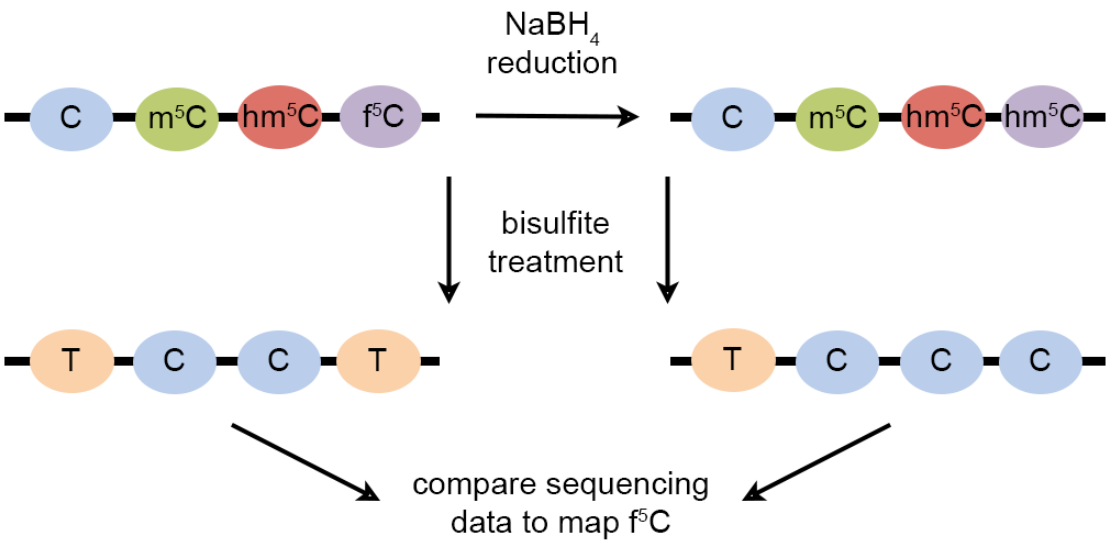

Figure 12: Reaction scheme of reduced and non-reduced bisulfite treatment of cytosines. Bisulfite treatment (BT) converts cytosine (C) and formylated cytosine (f^5C) to thymine (T), whereas methylated cytosine (m^5C) hydroxymethylated cytosine (hm^5C) remains cytosine. Reduced bisulfite treatment (RBT) uses $NaBH_4$ (sodium borohydride) to reduce f^5C to hm^5C, that acts like m^5C in following bisulfite treatment. By comparing sequencing data from BT with RBT, methylated and unmodified/formylated cytosine can be distinguished.
(Modified after Booth et al. 2014). With kind permission from Springer Nature.

To test which modification is present at position 34 of mt-$tRNA^{Met}$ in the presence or absence of ABH1 and demonstrate if ABH1 is necessary and therefore essential for conversion of m^5C to f^5C *in vivo*, RNA from cells treated

with a non-target siRNA or the established siRNAs against ABH1 were subjected to BT and RBT followed by Sanger sequencing.

Quantification of the number of sequencing reads containing a C or T at position 34 from control samples treated with a non-target siRNA showed almost exclusive presence of C after RBT, indicating C34 of mt-tRNA^{Met} is almost fully modified *in vivo*. The BT of the control showed approximately 60 % C and 40 % T, suggesting a mixture of methylated and unmodified/formylated cytosine on position 34 of mt-tRNA^{Met}, which by comparison to RBT data, would be interpreted as f^{5}C.

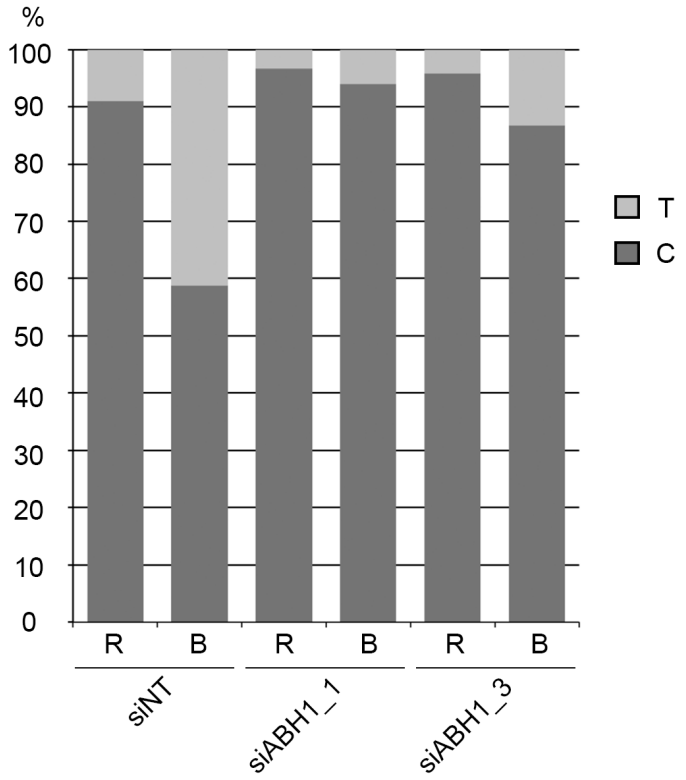

Figure 13: Deep sequencing data after reduced and non-reduced bisulfite treatment. Quantified sequence reads containing a cytosine (C) or thymine (T) at position 34 show almost exclusive C in reduced bisulfite treatment (R) of the control, suggesting that C34 of mt-tRNA^{Met} is almost fully modified *in vivo*, whereas bisulfite treatment (B) showed approximately 60 % C and 40 % T, suggesting a mixture of methylated and unmodified/formylated cytosine. Cells depleted of ABH1 bring out mostly C being detected with both BT and RBT, which corresponds to m^{5}C, showing that ABH1 converts m^{5}C34 to f^{5}C34 *in vivo*.

Interestingly, knock-down of ABH1 leads to mostly C being detected with both BT and RBT, which indicates the presence of m^{5}C at this position. Taken together, these results support the finding that ABH1 does convert m^{5}C34 to f^{5}C34 *in vivo*.

4 Discussion

4.1 Modification pathway of C34 of mt-tRNA^{Met}

4.1.1 Methylation by NSUN3

Epitranscriptomics is an emerging concept in the field of nucleotide modifications. In analogy to the well-established epigenetics field, where DNA and histone modifications influence gene activity and expression without affecting underlying DNA sequence, RNA modifications installed throughout the transcriptome can affect gene expression and gene expression regulation.

Although over the last years, more than one hundred types of RNA modifications where identified in all kinds of cellular RNAs, including mRNAs, rRNAs, tRNAs, micro RNAs (miRNAs), small nuclear (snRNAs) and long non-coding RNAs (lncRNAs), we still observe huge discrepancy between the wealth of mapping data and deeper understanding of their exact functions of many of these modifications and knowledge of the catalysing enzymes involved.

One well characterised nucleotide modification in DNA is the 5-methylation of cytosine, that has also been found in RNA, where it seems to have an influence on mRNA metabolism, tRNA stability and influences ribosome structure and function. However, a possible involvement in mitochondrial gene expression regulation has not been described yet. Enzymes that are responsible for installation of methyl groups on position 5 of cytosine residues in RNA are any of the seven proteins of the NSUN family (NSUN2 – 7) and the DNA methyltransferase 2 (DNMT2) (Bohnsack et al. 2019). Previous work from the Bohnsack lab showed that NSUN3 specifically interacts with mt-tRNA^{Met} (Haag et al. 2016). By use of the transcriptome-wide UV cross-linking and analysis of cDNA (CRAC) (Bohnsack et al. 2012; Sloan et al. 2015) and 5-azacytidine (5-AzaC) CRAC in HEK 293 cell lines, NSUN3 was found to chemically crosslink specifically to mt-tRNA^{Met}. Sub-cellular localisation studies confirmed NSUN3 to be localised in mitochondria, as previously discussed (Bujnicki et al. 2004). Confocal fluorescence microscopy and isolation studies of mitochondria of HEK 293 cell lines stably expressing green fluorescent protein (GFP)-tagged

NSUN3 then demonstrated its localisation in the mitochondrial matrix (Haag et al. 2016).

NSUN3's catalytic function in installation of methyl group on position 34 of cytosine was confirmed using *in vitro* methylation assays with recombinant NSUN3. Comparison to the lack of activity of a catalytically inactive mutant and lack of methylation on two other mt-tRNAs (mt-tRNA^{Pro} and mt-tRNA^{Glu}) demonstrated the specificity of its activity for mt-tRNA^{Met}. Remarkably, methylation assays with synthetic transcripts of the anticodon stem loop of mt-tRNA^{Met} further showed that this is sufficient for binding and methylation of NSUN3 (Haag et al. 2016).

4.1.2 ABH1 in the production of f^{5}C34 of mt-tRNA^{Met}

Interestingly, previous studies had suggested that the wobble position 34 of mt-tRNA^{Met} carries a formylated cytosine instead of m^{5}C (Moriya et al. 1994; Takemoto et al. 2009; Bilbille et al. 2011; Suzuki and Suzuki 2014). This f^{5}C, found in mt-tRNA^{Met} from vertebrates and nematodes was proposed to be responsible for unconventional decoding of AUA codon in mitochondria (Moriya et al. 1994; Watanabe et al. 1994; Suzuki et al. 2011; Nakano et al. 2016). Building on these data, the Bohnsack lab hypothesised that the m^{5}C in mt-tRNA^{Met} installed by NSUN3 is converted to f^{5}C.

Conversion of m^{5}C to f^{5}C would involve oxidation and enzymes that can do oxidation reactions are the so called AlkB family of proteins (Shen et al. 2014; Fedeles et al. 2015; Ougland et al. 2015). Based on its expected localisation in mitochondria, in this study, direct protein-RNA interaction analysis was performed to see if these proteins also bind mt-tRNA^{Met}. This was the case for ABH1 that was shown not to bind to mt-tRNA^{Glu} suggesting a specific interaction. In subsequent *in vitro* methylation and oxidation assays using recombinant wild type and catalytically inactive ABH1, I showed that ABH1 can convert m^{5}C34 to f^{5}C34 in mt-tRNA^{Met}. Importantly, no oxidation was observed in absence of pre-methylation by NSUN3, indicating a modification pathway of unmodified C34 to f^{5}C via m^{5}C, that relies on the sequential action of the two enzymes.

The role of ABH1 in making f^5C34 in mt-$tRNA^{Met}$ was also studied in cells. Knock-down of ABH1 in cells using RNAi was established here and I performed bisulfite sequencing (BS) to check the effect on f^5C34. This confirmed the *in vitro* results that ABH1 converts m^5C34 to f^5C34. After this study was conducted, the Bohnsack lab also verified ABH1's oxidative action on RNAs from cells by another method. RNAs from knock-downs of the two enzymes were treated with a 5-formylpyrimidine-specific label, 2,3,3-trimethylindolenin (TMI), which then acts to block reverse transcriptase activity at a modification site. This confirmed that there is less f^5C34 in mt-$tRNA^{Met}$ when cells lack ABH1 (Haag et al. 2016).

4.1.3 Relative amounts of m^5C and f^5C detected at position 34 of mt-$tRNA^{Met}$

Initial analysis of the modification state of C34 in mt-$tRNA^{Met}$ suggested exclusive formylation of the wobble position (Moriya et al. 1994; Bilbille et al. 2011; Suzuki et al. 2011; Suzuki and Suzuki 2014). The results of bisulfite and reduced bisulfite treatment followed by Sanger sequencing of this study show an almost exclusive presence of modified cytosine on position 34 of mt-$tRNA^{Met}$ but an equilibrium of approximately 60 % and methylated and 40 % formylated nucleotides. Interestingly, two other studies that were performed concurrently also found different ratios of methylated and formylated residues (Haute et al. 2016; Nakano et al. 2016).

I speculate that these differing results might be due to limitations of the methods that were used. While data uniquely detected f^5C was obtained using mass spectrometry, the other reports used BS to determine the modification status (m^5C, hm^5C, f^5C or unmodified cytosine) of the nucleotide of interest. In (reduced) BS, incomplete reduction of f^5C to hm^5C, which reads like m^5C could lead to more m^5C being detected, thus the actual proportion of f^5C34 in mature mt-$tRNA^{Met}$ might be higher.

To increase certainty of detection of f^5C in further research, a newly developed enzymatic demethylation approach could be implemented in BS where samples are methylated by a CpG methyltransferase (M.SssI) *in vitro* (Neri et al. 2016). After the treatment, all cytosine modifications except f^5C (and

5-carboxylcytosine) are methylated and can no longer undergo conversion to thymine in later bisulfite treatment.

It could also however be that the different ratios of modifications at the wobble position of mt-tRNA^{Met} depend on the cell type and their metabolic environment. This could be addressed in further studies by extraction of mt-tRNA^{Met} from different tissues, e.g. liver tissue, nervous tissue, embryonic stem cells and cancer cells in addition, combined with using the aforementioned techniques to monitor the modification status.

4.1.4 Function of f^{5}C in expanding codon recognition by mt-tRNA^{Met}

Potential effects of different modification states of mt-tRNA^{Met} C34 on mitochondrial translation has been matter of debate (Agris et al. 2007; Duechler et al. 2016; Ranjan and Rodnina 2016). Due to the lack of a reconstituted mitochondrial *in vitro* translation system, the Bohnsack lab established, together with the Rodnina lab (Department of Physical Biochemistry, Max Planck Institute for Biophysical Chemistry, Goettingen, Germany), binding assays involving chemically synthesised, differently modified mt-tRNA^{Met} (m^{5}C, hm^{5}C, f^{5}C and unmodified mt-tRNA^{Met}) and ribosomes from *E. coli* that were programmed with mRNAs containing either codon AUG, AUA or AUU. Despite significant structural differences of bacterial and mitoribosomes, the highly conserved decoding centres enable mimicking of (mito-)ribosomal translation by use of human mitochondrial translation factors, MTIF2 for translation initiation and TUFM for translation elongation, respectively (Greber and Ban 2016). Obtained data showed different affinity profiles with preference of m^{5}C for recognition of the universal AUG codon (or the AUA codon) during translation initiation while no preference between all tRNAs was observed during translation elongation (Haag et al. 2016). These results support that the modification state of C34 in mt-tRMA^{Met} affects codon recognition in mitochondrial translation. The Bohnsack lab also confirmed this by metabolic labelling of mitochondrial proteins in knock-downs of NSUN3 and ABH1 and found that lack of these proteins perturbs mitochondrial translation.

4.2 Target spectrum of ABH1

In this study, I demonstrated that ABH1 is part of a modification pathway that forms f^5C34 in mt-$tRNA^{Met}$. Previously, ABH1 had been reported to demethylate m^3C with substrate specificity for single-stranded DNA and RNA *in vitro* (Westbye et al. 2008). Independently, reports mentioned ABH1 to act as histone dioxygenase and cleave DNA at abasic sites (Müller et al. 2010; Ougland et al. 2012). These findings suggest ABH1 might have multiple targets in RNA, DNA and protein.

Interestingly, a recent study confirmed that ABH1 installs f^5C34 in mt-$tRNA^{Met}$ and demonstrated a biosynthetic pathway of f^5C34 over hm^5C34, where ABH1 first hydroxylises m^5C34 to form hm^5C34 and then, in a second step oxidises hm^5C34 to generate f^5C34. In the nucleus, they also found ABH1 to post-transcriptionally install f^5C on the wobble position 34 cytoplasmic tRNA Leucin, confirming previous reports that ABH1 also localises in the nucleus (Ougland et al. 2012; Kawarada et al. 2017). Another study recently reported ABH1 to act as an “eraser” enzyme on cytosolic mRNA in mammalian cells, it was found to demethylate m^3C in mRNA, further expanding the target spectrum of ABH1 (Ma et al. 2019). Together with data suggesting ABH1’s involvement in demethylation (m^1A) of several tRNAs (Liu et al. 2016), it shows that ABH1 not only recognises other modified nucleotides, but also that it performs different reactions on them.

A three-dimensional crystal structure of ABH1 would not only give insights about possible binding sites of their modified RNA substrates, but also, the question of the mechanistic basis of its different catalytic abilities and the molecular mechanics for the observed specificity of ABH1 in biosynthesis of f^5C in mt-$tRNA^{Met}$ in particular could be addressed. Therefore, performing crystallisation experiments of recombinant ABH1 purified from *E. coli* (as in this study) bound to its different substrates would be the next logical step to address all these questions.

4.3 Role of RNA modifications in co-ordinating cells response to metabolic status

The discovery of modifications in many types of RNA throughout the transcriptome, which were shown to have an impact on gene expression, was a major breakthrough in the RNA modification field that has led to the concept of epitranscriptomics. With “writer” enzymes that add chemical modifications, binding proteins that “read” modified nucleotides and “eraser” enzymes that can de-install the modifications, such RNA modifications are no longer seen as static, but are considered crucial in the dynamic regulation of cell homeostasis (Helm and Motorin 2017; Bohnsack and Sloan 2018).

Another emerging concept in the modification field is the discovery of the interrelation between dynamic RNA modifications and metabolic processes of the cell. Although changes in RNA modifications in response to changing environmental stimuli (e.g. temperature, exposure to UV light) have been already described in the early nineties, methodical difficulties in the qualitative and quantitative detection of RNA modifications had left the approaches for the most part descriptive (Emilsson et al. 1992; Kowalak et al. 1994; Helm and Alfonzo 2014; Liu et al. 2016; Bohnsack and Sloan 2018).

In the study, I present ABH1 as RNA dioxygenase that mediates oxidation of m^5C34 to f^5C34 in mt-$tRNA^{Met}$. In addition, we could confirm that ABH1 is only able to form f^5C34 in presence of cofactors α-ketoglutarate and iron (Fe^{2+}). This is especially relevant in this context as α-ketoglutarate is an important biological compound that participates in many metabolic processes in the cell of mammals and humans. It is a key nitrogen transporter in the cell, serves as cofactor of over 60 hydroxylases and oxygenases including the other members of the AlkB protein family of dioxygenases and it is also a powerful antioxidant (Loenarz and Schofield 2011; Long and Halliwell 2011; Walport et al. 2012; Markolovic et al. 2015; Salminen et al. 2015). α-ketoglutarate is also an important intermediate of the Krebs cycle, which takes place in mitochondria and is necessary for intracellular energy production by converting glucose to ATP. Accumulation of succinate, a metabolite of α-ketoglutarate, inhibits energy production, and could in consequence significantly affect the energy output of the cell (Haag et al. 2016; Neupert 2016). Much further work is needed however

to properly understand how exactly RNA modifications contribute to adaptation of cells in different metabolic conditions.

4.4 Mitochondrial tRNA modifications and disease

Interestingly, several studies have found mutations both in the genes encoding mt-tRNA^{Met} and the enzyme NSUN3 that is responsible for methylation of C34, presenting with a variety of clinical symptoms, some leading to impairment of mitochondrial function and severe clinical manifestations in humans (Lott et al. 2013; Haag et al. 2016; Nakano et al. 2016; Kawarada et al. 2017).

4.4.1 Pathogenic mutations in *NSUN3*

Whole exome sequencing (WES) data of a young patient presenting with combined developmental disability in the form of growth retardation and muscle weakness, microcephaly, ophthalmoplegia and high blood lactate levels revealed compound heterozygous loss of function mutations in *NSUN3*. In compound heterozygosity, both alleles are affected by the mutation, in this case, deletion of Exon 3 of the maternal allele (c.123-615_466 þ 2155del) and point mutation (c.295C4T) of the paternal allele, both leading to dysfunctional protein fragment(s) of the methyltransferase NSUN3. Analysis of muscle tissue showed significant decrease of OXPHOS complex activity, and testing of fibroblasts derived from the patient confirmed expression of a shortened, dysfunctional NSUN3 protein. Compromised mitochondrial respiratory chain activity that was detected by reduced oxygen consumption and decreased growth rate when cells are forced to rely more on mitochondrial ATP production from galactose, was restored by exogenous expression of NSUN3 from cDNA introduced by lentiviral transduction (Haute et al. 2016). The authors therefore conclude that lack of functioning NSUN3 hindered mitochondrial protein synthesis. The decreased decoding efficacy of the unmodified mt-tRNA^{Met} caused deficiency of the OXPHOS system ultimately leading to deficient cellular respiration and the described mitochondrial disease symptoms.

4.4.2 Pathogenic mutations identified in mt-tRNA^{Met}

Physiological manifestations of mutations in mtDNA and their clinical correlates are very heterogeneous, which can be explained by mitochondrial heteroplasmy

(mitochondria containing multiple genomes per cell). Remarkably, even though pathogenic point-mutation of mt-tRNA account only 5 – 10 % of total mtDNA sequence, they are responsible for most of mtDNA diseases (Anderson et al. 1981; Yarham et al. 2010). Interestingly, two (A4435G and C4437U) of the eight mapped *mt-tRNA^{Met}* mutations reported so far were shown to significantly decrease methylation activity by NSUN3 *in vitro*. Both point mutations lead to nucleotide substitutions that are located in the anticodon stem loop region of mt-tRNA^{Met} and seem to weaken interaction of mt-tRNA^{Met} and NSUN3 during methylation of C34. Pathogenic point mutation A443G was found in patients suffering from maternally inherited hypertension, while patients carrying C4437U reported muscle weakness, hypotonia, seizures, hearing loss and lactic acidosis (Yarham et al. 2010; Lu et al. 2011; Nakano et al. 2016).

Together, these findings further underline the importance of the wobble position of mt-tRNAs as epitranscriptomic hotspot and that lack of modifications at this position can be responsible for mitochondrial syndromes.

It is conceivable that with the broader accessibility of WES of material from patients presenting with mitochondrial disease symptoms, further mutations in *NSUN3* will be found that have an effect on its function. It remains to be seen if pathogenic mutations in *ABH1* also exist, which have an effect on its function in wobble base modification of mt-tRNA^{Met}.

On a wider level, additional steps could be taken to elucidate the physiological and pathophysiological relevance of *NSUN3* and *ABH1*. For this, it would be interesting to create a knock-out system in an animal model where both developmental and disease phenotypes could be analysed in more detail.

5 Summary

Ribonucleic acid (RNA) modifications have been found in all coding and non-coding RNAs and represent a key mechanism in the homeostatic control of cell metabolism including gene expression and regulation. Therefore, the wobble base cytosine on position 34 (C34) of mitochondrial initiator and elongator transfer RNA methionine (mt-tRNA^{Met}), that allows non-conventional codon-anticodon base pairing, may be of superior importance. Literature suggested a 5-formylated residue on C34 of mt-tRNA^{Met} and the Bohnsack lab could identify methyltransferase NSUN3 to interact with and install m^{5}C of mt-tRNA^{Met}. However, the conversion to f^{5}C34 and the enzyme involved remained unclear. The dioxygenase ABH1, that has been shown to localise to mitochondria, represents a potential candidate and its activity in the oxidation of m^{5}C34 was my subject of investigation.

RNA immunoprecipitation (RNA-IP) experiments after UV crosslinking followed by northern blotting and ethidium bromide staining of mt-tRNA^{Met} and ABH1 were performed. Recombinant expression of ABH1 and catalytically inactive mutants, created by site-directed mutagenesis, was established in *E. coli*. The purified proteins were used in *in vitro* methylation and oxidation assays involving radioactive ^{3}H (tritium). Sufficient depletion of ABH1 in human embryonic kidney 293 (HEK 293) cells was carried out by RNA interference (RNAi) and the modification status of C34 of mt-tRNA^{Met} was monitored after bisulfite and reduced bisulfite treatment followed by Sanger sequencing.

Taken together, I could identify ABH1 to specifically interact with mt-tRNA^{Met}. Furthermore, I was able to monitor oxidation of m^{5}C34 of mt-tRNA^{Met} by recombinant ABH1 *in vitro*. ABH1 could be efficiently depleted by RNAi in Henrietta Lacks CCL2 (HeLa CCL2) human cervical carcinoma cells and a sequential modification pattern of unmodified mt-tRNA^{Met} C34 to m^{5}C34 by NSUN3, followed by ABH1 mediated oxidation to f^{5}C34, could be described *in vivo*.

ABH1 is an active enzyme capable of oxidising m^{5}C into f^{5}C and this activity is responsible for generating the f^{5}C34 present in mt-tRNA^{Met} in cells. Its target

spectrum, the role of mt-tRNA^{Met} C34 as epitranscriptomic hotspot and their involvement in pathologic metabolic processes in human cells are questions that need to be addressed in further research.

6 References

Abbasi-Moheb L, Mertel S, Gonsior M, Nouri-Vahid L, Kahrizi K, Cirak S, Wieczorek D, Motazacker MM, Esmaeeli-Nieh S, Cremer K et al. (2012): Mutations in NSUN2 cause autosomal-recessive intellectual disability. Am J Hum Genet 90, 847-855

Agris PF, Vendeix F, Graham WD (2007): tRNA's wobble decoding of the genome: 40 years of modification. J Mol Biol 366, 1-13

Alexandrov A, Chernyakov I, Gu W, Hiley SL, Hughes TR, Grayhack EJ, Phizicky EM (2006): Rapid tRNA decay can result from lack of nonessential modifications. Mol Cell 21, 87-96

Amunts A, Brown A, Toots J, Scheres SHW, Ramakrishnan V (2015): The structure of the human mitochondrial ribosome. Science 348, 95-98

Anderson S, Bankier AT, Barrell BG, de Bruijn MH, Coulson AR, Drouin J, Eperon IC, Nierlich DP, Roe BA, Sanger F et al. (1981): Sequence and organization of the human mitochondrial genome. Nature 290, 457-465

Baruffini E, Dallabona C, Invernizzi F, Yarham JW, Melchionda L, Blakely EL, Lamantea E, Donnini C, Santra S, Vijayaraghavan S et al. (2013): MTO1 mutations are associated with hypertrophic cardiomyopathy and lactic acidosis and cause respiratory chain deficiency in humans and yeast. Hum Mutat 34, 1501-1509

Bar-Yaacov D, Frumkin I, Yashiro Y, Chujo T, Ishigami Y, Chemla Y, Blumberg A, Schlesinger O, Bieri P, Greber B et al. (2017): Correction: Mitochondrial 16S rRNA is methylated by tRNA methyltransferase TRMT61B in all vertebrates. PLoS Biol 15, e1002594

Bednářová A, Hanna M, Durham I, VanCleave T, England A, Chaudhuri A, Krishnan N (2017): Lost in translation: defects in transfer RNA modifications and neurological disorders. Front Mol Neurosci 10, 135

Bilbille Y, Gustilo EM, Harris KA, Jones CN, Lusic H, Kaiser RJ, Delaney MO, Spremulli LL, Deiters A, Agris PF (2011): The human mitochondrial tRNAMet: structure/function relationship of a unique modification in the decoding of unconventional codons. J Mol Biol 406, 257-274

Blanchard SC, Puglisi JD (2001): Solution structure of the A loop of 23S ribosomal RNA. Proc Natl Acad Sci U S A 98, 3720-3725

Blanco S, Frye M (2014): Role of RNA methyltransferases in tissue renewal and pathology. Curr Opin Cell Biol 31, 1-7

Blanco S, Dietmann S, Flores JV, Hussain S, Kutter C, Humphreys P, Lukk M, Lombard P, Treps L, Popis M et al. (2014): Aberrant methylation of tRNAs links cellular stress to neuro-developmental disorders. EMBO J 33, 2020-2039

Bleijlevens B, Shivarattan T, van den Boom KS, de Haan A, van der Zwan G, Simpson PJ, Matthews SJ (2012): Changes in protein dynamics of the DNA repair dioxygenase AlkB upon binding of fe(2+) and 2-oxoglutarate. Biochemistry 51, 3334-3341

Boccaletto P, Machnicka MA, Purta E, Piatkowski P, Baginski B, Wirecki TK, de Crécy-Lagard V, Ross R, Limbach PA, Kotter A et al. (2018): MODOMICS: a database of RNA modification pathways. 2017 update. Nucleic Acids Res 46, D303-D307

Bohnsack KE, Höbartner C, Bohnsack MT (2019): Eukaryotic 5-methylcytosine (m5C) RNA methyltransferases: mechanisms, cellular functions, and links to disease. Genes (Basel) 10, 102

Bohnsack MT, Sloan KE (2018): The mitochondrial epitranscriptome: the roles of RNA modifications in mitochondrial translation and human disease. Cell Mol Life Sci 75, 241-260

Bohnsack MT, Tollervey D, Granneman S (2012): Identification of RNA helicase target sites by UV cross-linking and analysis of cDNA. Methods Enzymol 511, 275-288

Booth MJ, Marsico G, Bachman M, Beraldi D, Balasubramanian S (2014): Quantitative sequencing of 5-formylcytosine in DNA at single-base resolution. Nat Chem 6, 435-440

Bradford MM (1976): A rapid and sensitive method for the quantitation of microgram quantities of protein utilizing the principle of protein-dye binding. Anal Biochem 72, 248-254

Breiling A, Lyko F (2015): Epigenetic regulatory functions of DNA modifications: 5-methylcytosine and beyond. Epigenetics Chromatin 8, 24

Brulé H, Elliott M, Redlak M, Zehner ZE, Holmes WM (2004): Isolation and characterization of the human tRNA-(N1G37) methyltransferase (TRM5) and comparison to the Escherichia coli TrmD protein. Biochemistry 43, 9243-9255

Bujnicki JM, Feder M, Ayres CL, Redman KL (2004): Sequence-structure-function studies of tRNA:m5C methyltransferase Trm4p and its relationship to DNA:m5C and RNA:m5U methyltransferases. Nucleic Acids Res 32, 2453-2463

Cámara Y, Asin-Cayuela J, Park CB, Metodiev MD, Shi Y, Ruzzenente B, Kukat C, Habermann B, Wibom R, Hultenby K et al. (2011): MTERF4 regulates translation by targeting the methyltransferase NSUN4 to the mammalian mitochondrial ribosome. Cell Metab 13, 527-539

Carlile TM, Rojas-Duran MF, Zinshteyn B, Shin H, Bartoli KM, Gilbert WV (2014): Pseudouridine profiling reveals regulated mRNA pseudouridylation in yeast and human cells. Nature 515, 143-146

Chan C, Pang Y, Deng W, Babu RI, Dyavaiah M, Begley TJ, Dedon PC (2012): Reprogramming of tRNA modifications controls the oxidative stress response by codon-biased translation of proteins. Nat Commun 3, 937

Chen Z, Qi M, Shen B, Luo G, Wu Y, Li J, Lu Z, Zheng Z, Dai Q, Wang H (2018): Transfer RNA demethylase ALKBH3 promotes cancer progression via induction of tRNA-derived small RNAs. Nucleic Acids Res 47, 2533-2345

Chi L, Delgado-Olguín P (2013): Expression of NOL1/NOP2/sun domain (Nsun) RNA methyltransferase family genes in early mouse embryogenesis. Gene Expr Patterns 13, 319-327

Davarniya B, Hu H, Kahrizi K, Musante L, Fattahi Z, Hosseini M, Maqsoud F, Farajollahi R, Wienker TF, Ropers HH et al. (2015): The role of a novel TRMT1 gene mutation and rare GRM1 gene defect in intellectual disability in two azeri families. PLoS One 10, e0129631

Davis DR (1995): Stabilization of RNA stacking by pseudouridine. Nucleic Acids Res 23, 5020-5026

Decatur WA, Fournier MJ (2002): rRNA modifications and ribosome function. Trends Biochem Sci 27, 344-351

Deng W, Babu IR, Su D, Yin S, Begley TJ, Dedon PC (2015): Trm9-catalyzed tRNA modifications regulate global protein expression by codon-biased translation. PLoS Genet 11, e1005706

Dominissini D (2014): Roadmap to the epitranscriptome. Science 346, 1192

Dominissini D, Moshitch-Moshkovitz S, Schwartz S, Salmon-Divon M, Ungar L, Osenberg S, Cesarkas K, Jacob-Hirsch J, Amariglio N, Kupiec M et al. (2012): Topology of the human and mouse m6A RNA methylomes revealed by m6A-seq. Nature 485, 201-206

Dorn GW 2nd, Vega RB, Kelly DP (2015): Mitochondrial biogenesis and dynamics in the developing and diseased heart. Genes Dev 29, 1981-1991

Duechler M, Leszczyńska G, Sochacka E, Nawrot B (2016): Nucleoside modifications in the regulation of gene expression: focus on tRNA. Cell Mol Life Sci 73, 3075-3095

Duncan T, Trewick SC, Koivisto P, Bates PA, Lindahl T, Sedgwick B (2002): Reversal of DNA alkylation damage by two human dioxygenases. Proc Natl Acad Sci U S A 99, 16660-16665

El Yacoubi B, Bailly M, de Crécy-Lagard V (2012): Biosynthesis and function of posttranscriptional modifications of transfer RNAs. Annu Rev Genet 46, 69-95

Emilsson V, Näslund AK, Kurland CG (1992): Thiolation of transfer RNA in Escherichia coli varies with growth rate. Nucleic Acids Res 20, 4499-4505

Fahiminiya S, Almuriekhi M, Nawaz Z, Staffa A, Lepage P, Ali R, Hashim L, Schwartzentruber J, Khadija KA, Zaineddin S et al. (2014): Whole exome sequencing unravels disease-causing genes in consanguineous families in qatar. Clin Genet 86, 134-141

Falaleeva M, Pages A, Matuszek Z, Hidmi S, Agranat-Tamir L, Korotkov K, Nevo Y, Eyras E, Sperling R, Stamm S (2016): Dual function of C/D box small nucleolar RNAs in rRNA modification and alternative pre-mRNA splicing. Proc Natl Acad Sci U S A 113, E1625-E1634

Fedeles BI, Singh V, Delaney JC, Li D, Essigmann JM (2015): The AlkB family of fe(II)/α-ketoglutarate-dependent dioxygenases: repairing nucleic acid alkylation damage and beyond. J Biol Chem 290, 20734-20742

Frye M, Watt FM (2006): The RNA methyltransferase misu (NSun2) mediates Myc-induced proliferation and is upregulated in tumors. Curr Biol 16, 971-981

Fu Y, Dai Q, Zhang W, Ren J, Pan T, He C (2010): The alkB domain of mammalian ABH8 catalyzes hydroxylation of 5-methoxycarbonylmethyluridine at the wobble position of tRNA. Angew Chem Int Ed Engl 49, 8885-8888

Gardner A, Boles RG (2005): Is a “mitochondrial psychiatry” in the future? A review. Curr Psychiatry Rev 1, 255-271

Ghezzi D, Baruffini E, Haack TB, Invernizzi F, Melchionda L, Dallabona C, Strom TM, Parini R, Burlina AB, Meitinger T et al. (2012): Mutations of the mitochondrial-tRNA modifier MTO1 cause hypertrophic cardiomyopathy and lactic acidosis. Am J Hum Genet 90, 1079-1087

Goll MG, Kirpekar F, Maggert KA, Yoder JA, Hsieh CL, Zhang X, Golic KG, Jacobsen SE, Bestor TH (2006): Methylation of tRNAAsp by the DNA methyltransferase homolog Dnmt2. Science 311, 395-398

Goto Y, Nonaka I, Horai S (1990): A mutation in the tRNA(Leu)(UUR) gene associated with the MELAS subgroup of mitochondrial encephalomyopathies. Nature 348, 651-653

Greber BJ, Ban N (2016): Structure and function of the mitochondrial ribosome. Annu Rev Biochem 85, 103-132

Green R, Noller HF (1999): Reconstitution of functional 50S ribosomes from in vitro transcripts of bacillus stearothermophilus 23S rRNA. Biochemistry 38, 1772-1779

Grosjean H, Westhof E (2016): An integrated, structure- and energy-based view of the genetic code. Nucleic Acids Res 44, 8020-8040

Haag S, Warda AS, Kretschmer J, Günnigmann MA, Höbartner C, Bohnsack MT (2015): NSUN6 is a human RNA methyltransferase that catalyzes formation of m5C72 in specific tRNAs. RNA 21, 1532-1543

Haag S, Sloan KE, Ranjan N, Warda AS, Kretschmer J, Blessing C, Hübner B, Seikowski J, Dennerlein S, Rehling P et al. (2016): NSUN3 and ABH1 modify the wobble position of mt-tRNAMet to expand codon recognition in mitochondrial translation. EMBO J 35, 2104-2119

Hall KB, Sampson JR, Uhlenbeck OC, Redfield AG (1989): Structure of an unmodified tRNA molecule. Biochemistry 28, 5794-5801

Hällberg BM, Larsson NG (2014): Making proteins in the powerhouse. Cell Metab 20, 226-240

Haute LV, Dietmann S, Kremer L, Hussain S, Pearce SF, Powell CA, Rorbach J, Lantaff R, Blanco S, Sauer S et al. (2016): Deficient methylation and formylation of mt-tRNA(Met) wobble cytosine in a patient carrying mutations in NSUN3. Nat Commun. 7, 12039

He YF, Li BZ, Li Z, Liu P, Wang Y, Tang Q, Ding J, Jia Y, Chen Z, Li L et al. (2011): Tet-mediated formation of 5-carboxylcytosine and its excision by TDG in mammalian DNA. Science 333, 1303-1307

Helm M, Alfonzo JD (2014): Posttranscriptional RNA modifications: playing metabolic games in a cell's chemical legoland. Chem Biol 21, 174-185

Helm M, Motorin Y (2017): Detecting RNA modifications in the epitranscriptome: predict and validate. Nat Rev Genet 18, 275-291

Hess ME, Hess S, Meyer KD, Verhagen LA, Koch L, Brönneke HS, Dietrich MO, Jordan SD, Saletore Y, Elemento O et al. (2013): The fat mass and obesity associated gene (Fto) regulates activity of the dopaminergic midbrain circuitry. Nat Neurosci 16, 1042-1048

Hopper AK (2013): Transfer RNA post-transcriptional processing, turnover, and subcellular dynamics in the yeast Saccharomyces cerevisiae. Genetics 194, 43-67

Hörbartner C, Ebert MO, Jaun B, Micura R (2002): RNA two-state conformation equilibria and the effect of nucleobase methylation. Angew Chem 41, 605-609

Hussain S, Sajini AA, Blanco S, Dietmann S, Lombard P, Sugimoto Y, Paramor M, Gleeson JG, Odom DT, Ule J et al. (2013): NSun2-mediated cytosine-5 methylation of vault noncoding RNA determines its processing into regulatory small RNAs. Cell Rep 4, 255-261

Ito S, Shen L, Dai Q, Wu SC, Collins LB, Swenberg JA, He C, Zhang Y (2011): Tet proteins can convert 5-methylcytosine to 5-formylcytosine and 5-carboxylcytosine. Science 333, 1300-1303

Jia G, Fu Y, Zhao X, Dai Q, Zheng G, Yang Y, Yi C, Lindahl T, Pan T, Yang YG et al. (2011): N6-methyladenosine in nuclear RNA is a major substrate of the obesity-associated FTO. Nat Chem Biol 7, 885-887

Jonkhout N, Tran J, Smith MA, Schonrock N, Mattick JS, Novoa EM (2017): The RNA modification landscape in human disease. RNA 23, 1754-1769

Jorjani H, Kehr S, Jedlinski DJ, Gumienny R, Hertel J, Stadler PF, Zavolan M, Gruber AR (2016): An updated human snoRNAome. Nucleic Acids Res 44, 5068-5082

Kawarada L, Suzuki T, Ohira T, Hirata S, Miyauchi K, Suzuki T (2017): ALKBH1 is an RNA dioxygenase responsible for cytoplasmic and mitochondrial tRNA modifications. Nucleic Acids Res 45, 7401-7415

Khaitovich P, Tenson T, Kloss P, Mankin AS (1999): Reconstitution of functionally active thermus aquaticus large ribosomal subunits with in vitro-transcribed rRNA. Biochemistry 38, 1780-1788

Khan MA, Rafiq MA, Noor A, Hussain S, Flores JV, Rupp V, Vincent AK, Malli R, Ali G, Khan F et al. (2012): Mutation in NSUN2, which encodes an RNA methyltransferase, causes autosomal-recessive intellectual disability. Am J Hum Genet 90, 856-863

Kirino Y, Goto Y, Campos Y, Arenas J, Suzuki T (2005): Specific correlation between the wobble modification deficiency in mutant tRNAs and the clinical features of a human mitochondrial disease. Proc Natl Acad Sci U S A 102, 7127-7132

Kobayashi Y, Momoi MY, Tominaga K, Momoi T, Nihei K, Yanagisawa M, Kagawa Y, Ohta S (1990): A point mutation in the mitochondrial tRNA(Leu)(UUR) gene in MELAS (mitochondrial myopathy, encephalopathy,

lactic acidosis and stroke-like episodes). Biochem Biophys Res Commun 173, 816-822

Koeck T, Olsson AH, Nitert MD, Sharoyko VV, Ladenvall C, Kotova O, Reiling E, Rönn T, Parikh H, Taneera J et al. (2011): A common variant in TFB1M is associated with reduced insulin secretion and increased future risk of type 2 diabetes. Cell Metab 13, 80-91

Kopajtich R, Nicholls TJ, Rorbach J, Metodiev MD, Freisinger P, Mandel H, Vanlander A, Ghezzi D, Carrozzo R, Taylor RW et al. (2014): Mutations in GTPBP3 cause a mitochondrial translation defect associated with hypertrophic cardiomyopathy, lactic acidosis, and encephalopathy. Am J Hum Genet 95, 708-720

Kowalak JA, Dalluge JJ, McCloskey JA, Stetter KO (1994): The role of posttranscriptional modification in stabilization of transfer RNA from hyperthermophiles. Biochemistry 33, 7869-7876

Laemmli UK (1970): Cleavage of structural proteins during the assembly of the head of bacteriophage T4. Nature 227, 680-685

Lafontaine DL, Preiss T, Tollervey D (1998): Yeast 18S rRNA dimethylase Dim1p: a quality control mechanism in ribosome synthesis? Mol Cell Biol 18, 2360-2370

Lang BF, Gray MW, Burger G (1999): Mitochondrial genome evolution and the origin of eukaryotes. Annu Rev Genet 33, 351-397

Lee KW, Bogenhagen DF (2014): Assignment of 2′-O-methyltransferases to modification sites on the mammalian mitochondrial large subunit 16 S ribosomal RNA (rRNA). J Biol Chem 289, 24936-24942

Lee KW, Okot-Kotber C, LaComb JF, Bogenhagen DF (2013): Mitochondrial ribosomal RNA (rRNA) methyltransferase family members are positioned to modify nascent rRNA in foci near the mitochondrial DNA nucleoid. J Biol Chem 288, 31386-31399

Li MM, Nilsen A, Shi Y, Fusser M, Ding YH, Fu Y, Liu B, Niu Y, Wu YS, Huang CM et al. (2013): ALKBH4-dependent demethylation of actin regulates actomyosin dynamics. Nat. Commun. 4, 1832

Liang XH, Liu Q, Fournier MJ (2007): rRNA modifications in an intersubunit bridge of the ribosome strongly affect both ribosome biogenesis and activity. Mol Cell 28, 965-977

Liang XH, Liu Q, Fournier MJ (2009): Loss of rRNA modifications in the decoding center of the ribosome impairs translation and strongly delays pre-rRNA processing. RNA 15, 1716-1728

Lin S, Choe J, Du P, Triboulet R, Gregory RI (2016): The m(6)A methyltransferase METTL3 promotes translation in human cancer cells. Mol Cell 62, 335-345

Liu F, Clark W, Luo G, Wang Xiaoy, Fu Y, Wei J, Wang Xiao, Hao Z, Dai Q, Zheng G et al. (2016): ALKBH1-mediated tRNA demethylation regulates translation. Cell 167, 816-828.e16

Loenarz C, Schofield CJ (2011): Physiological and biochemical aspects of hydroxylations and demethylations catalyzed by human 2-oxoglutarate oxygenases. Trends Biochem Sci 36, 7-18

Long LH, Halliwell B (2011): Artefacts in cell culture: α-ketoglutarate can scavenge hydrogen peroxide generated by ascorbate and epigallocatechin gallate in cell culture media. Biochem Biophys Res Commun 406, 20-24

Lott MT, Leipzig JN, Derbeneva O, Xie MH, Chalkia D, Sarmady M, Procaccio V, Wallace DC (2013): mtDNA variation and analysis using mitomap and mitomaster. Curr Protoc Bioinformatics. 44, 1.23.1-1.23.26

Lu Z, Chen H, Meng Y, Wang Y, Xue L, Zhi S, Qiu Q, Yang L, Mo J, Guan MX (2011): The tRNAMet 4435A>G mutation in the mitochondrial haplogroup G2a1 is responsible for maternally inherited hypertension in a chinese pedigree. Eur J Hum Genet 19, 1181-1186

Ma CJ, Ding JH, Ye TT, Yuan BF, Feng YQ (2019): AlkB Homologue 1 demethylates N3-methylcytidine in mRNA of mammals. ACS Chem Biol 14, 1418-1425

Mangum JE, Hardee JP, Fix DK, Puppa MJ, Elkes J, Altomare D, Bykhovskaya Y, Campagna DR, Schmidt PJ, Sendamarai AK et al. (2016): Pseudouridine synthase 1 deficient mice, a model for mitochondrial myopathy with

sideroblastic anemia, exhibit muscle morphology and physiology alterations. Sci Rep 6, 26202

Markolovic S, Wilkins SE, Schofield CJ (2015): Protein hydroxylation catalyzed by 2-oxoglutarate-dependent oxygenases. J Biol Chem 290, 20712-20722

Martinez FJ, Lee JH, Lee JE, Blanco S, Nickerson E, Gabriel S, Frye M, Al-Gazali L, Gleeson JG (2012): Whole exome sequencing identifies a splicing mutation in NSUN2 as a cause of a Dubowitz-like syndrome. J Med Genet 49, 380-385

McBride HM, Neuspiel M, Wasiak S (2006): Mitochondria: more than just a powerhouse. Curr Biol 16, R551-R560

Mei L, Shen C, Miao R, Wang JZ, Cao MD, Zhang YS, Shi LH, Zhao GH, Wang MH, Wu LS et al. (2020): RNA methyltransferase NSUN2 promotes gastric cancer cell proliferation by repressing p57Kip2 by an m5C-dependent manner. Cell Death Dis 11, 270

Metodiev MD, Lesko N, Park CB, Cámara Y, Shi Y, Wibom R, Hultenby K, Gustafsson CM, Larsson NG (2009): Methylation of 12S rRNA is necessary for in vivo stability of the small subunit of the mammalian mitochondrial ribosome. Cell Metab 9, 386-397

Metodiev MD, Spåhr H, Polosa PL, Meharg C, Becker C, Altmueller J, Habermann B, Larsson NG, Ruzzenente B (2014): NSUN4 is a dual function mitochondrial protein required for both methylation of 12S rRNA and coordination of mitoribosomal assembly. PLoS Genet 10, e1004110

Mokranjac D, Neupert W (2005): Protein import into mitochondria. Biochem Soc Trans 33, 1019-1023

Moriya J, Yokogawa T, Wakita K, Ueda T, Nishikawa K, Crain PF, Hashizume T, Pomerantz SC, McCloskey JA, Kawai G et al. (1994): A novel modified nucleoside found at the first position of the anticodon of methionine tRNA from bovine liver mitochondria. Biochemistry 33, 2234-2239

Motorin Y, Helm M (2010): tRNA stabilization by modified nucleotides. Biochemistry 49, 4934-4944

Müller TA, Meek K, Hausinger RP (2010): Human AlkB homologue 1 (ABH1) exhibits DNA lyase activity at abasic sites. DNA Repair (Amst.) 9, 58-65

Mullis K, Faloona F, Scharf S, Saiki R, Horn G, Erlich H (1992): Specific enzymatic amplification of DNA in vitro: the polymerase chain reaction. Biotechnology 24, 17-27

Nakano S, Suzuki Ta, Kawarada L, Iwata H, Asano K, Suzuki Ts (2016): NSUN3 methylase initiates 5-formylcytidine biogenesis in human mitochondrial tRNA(Met). Nat Chem Biol 12, 546-551

Napoli E, Wong S, Hertz-Picciotto I, Giulivi C (2014): Deficits in bioenergetics and impaired immune response in granulocytes from children with autism. Pediatrics 133, e1405-e1410

Nedialkova DD, Leidel SA (2015): Optimization of codon translation rates via tRNA modifications maintains proteome integrity. Cell 161, 1606-1618

Neri F, Incarnato D, Krepelova A, Parlato C, Oliviero S (2016): Methylation-assisted bisulfite sequencing to simultaneously map 5fC and 5caC on a genome-wide scale for DNA demethylation analysis. Nat Protoc 11, 1191-1205

Neupert W (2016): Mitochondrial gene expression: a playground of evolutionary tinkering. Annu Rev Biochem 85, 65-76

Oh-hama T (1997): Evolutionary consideration on 5-aminolevulinate synthase in nature. Orig Life Evol Biosph 27, 405-412

Ott M, Amunts A, Brown A (2016): Organization and regulation of mitochondrial protein synthesis. Annu Rev Biochem 85, 77-101

Ougland R, Lando D, Jonson I, Dahl JA, Moen MN, Nordstrand LM, Rognes T, Lee JT, Klungland A, Kouzarides T et al. (2012): ALKBH1 is a histone H2A dioxygenase involved in neural differentiation. Stem Cells 30, 2672-2682

Ougland R, Rognes T, Klungland A, Larsen E (2015): Non-homologous functions of the AlkB homologs. J Mol Cell Biol 7, 494-504

Patil A, Chan CT, Dyavaiah M, Rooney JP, Dedon PC, Begley TJ (2012): Translational infidelity-induced protein stress results from a deficiency in Trm9-catalyzed tRNA modifications. RNA Biol 9, 990-1001

Patton JR, Bykhovskaya Y, Mengesha E, Bertolotto C, Fischel-Ghodsian N (2005): Mitochondrial myopathy and sideroblastic anemia (MLASA): missense mutation in the pseudouridine synthase 1 (PUS1) gene is associated with the loss of tRNA pseudouridylation. J Biol Chem 280, 19823-19828

Paul MS, Bass BL (1998): Inosine exists in mRNA at tissue-specific levels and is most abundant in brain mRNA. EMBO J 17, 1120-1127

Persson BC, Esberg B, Olafsson O, Björk GR (1994): Synthesis and function of isopentenyl adenosine derivatives in tRNA. Biochimie 76, 1152-1160

Piekna-Przybylska D, Decatur WA, Fournier MJ (2008): The 3D rRNA modification maps database: with interactive tools for ribosome analysis. Nucleic Acids Res 36, D178-D183

Powell CA, Kopajtich R, D'Souza AR, Rorbach J, Kremer LS, Husain RA, Dallabona C, Donnini C, Alston CL, Griffin H et al. (2015): TRMT5 mutations cause a defect in post-transcriptional modification of mitochondrial tRNA associated with multiple respiratory-chain deficiencies. Am J Hum Genet 97, 319-328

Ranjan N, Rodnina MV (2016): tRNA wobble modifications and protein homeostasis. Translation (Austin) 4, e1143076

Ringvoll J, Moen MN, Nordstrand LM, Meira LB, Pang B, Bekkelund A, Dedon PC, Bjelland S, Samson LD, Falnes PØ et al. (2008): AlkB homologue 2-mediated repair of ethenoadenine lesions in mammalian DNA. Cancer Res 68, 4142-4149

Rorbach J, Minczuk M (2012): The post-transcriptional life of mammalian mitochondrial RNA. Biochem J 444, 357-373

Rorbach J, Boesch P, Gammage PA, Nicholls TJ, Pearce SF, Patel D, Hauser A, Perocchi F, Minczuk M (2014): MRM2 and MRM3 are involved in biogenesis of the large subunit of the mitochondrial ribosome. Mol Biol Cell 25, 2542-2555

Roundtree IA, Evans ME, Pan T, He C (2017): Dynamic RNA modifications in gene expression regulation. Cell 169, 1187-1200

Rozanska A, Richter-Dennerlein R, Rorbach J, Gao F, Lewis RJ, Chrzanowska-Lightowlers ZM, Lightowlers RN (2017): The human RNA-binding protein RBFA

promotes the maturation of the mitochondrial ribosome. Biochem J 474, 2145-2158

Salminen A, Kauppinen A, Kaarniranta K (2015): 2-Oxoglutarate-dependent dioxygenases are sensors of energy metabolism, oxygen availability, and iron homeostasis: potential role in the regulation of aging process. Cell Mol Life Sci 72, 3897-3914

Schaefer M, Pollex T, Hanna K, Tuorto F, Meusburger M, Helm M, Lyko F (2010): RNA methylation by Dnmt2 protects transfer RNAs against stress-induced cleavage. Genes Dev 24, 1590-1595

Schosserer M, Minois N, Angerer TB, Amring M, Dellago H, Harreither E, Calle-Perez A, Pircher A, Gerstl MP, Pfeifenberger S et al. (2015): Methylation of ribosomal RNA by NSUN5 is a conserved mechanism modulating organismal lifespan. Nat Commun 6, 6158

Shen L, Song CX, He C, Zhang Y (2014): Mechanism and function of oxidative reversal of DNA and RNA methylation. Annu Rev Biochem 83, 585-614

Shutt TE, Shadel GS (2010): A compendium of human mitochondrial gene expression machinery with links to disease. Environ Mol Mutagen 51, 360-379

Sloan KE, Bohnsack MT, Watkins NJ (2013): The 5S RNP couples p53 homeostasis to ribosome biogenesis and nucleolar stress. Cell Rep 5, 237-247

Sloan KE, Leisegang MS, Doebele C, Ramírez AS, Simm S, Safferthal C, Kretschmer J, Schorge T, Markoutsa S, Haag S et al. (2015): The association of late-acting snoRNPs with human pre-ribosomal complexes requires the RNA helicase DDX21. Nucleic Acids Res 43, 553-564

Sloan KE, Warda AS, Sharma S, Entian KD, Lafontaine DLJ, Bohnsack MT (2017): Tuning the ribosome: the influence of rRNA modification on eukaryotic ribosome biogenesis and function. RNA Biol 14, 1138-1152

Song J, Yi C (2017): Chemical modifications to RNA: a new layer of gene expression regulation. ACS Chem Biol 12, 316-325

Söll D (1971): Enzymatic modification of transfer RNA. Science 173, 293-299

Spåhr H, Habermann B, Gustafsson CM, Larsson NG, Hallberg BM (2012): Structure of the human MTERF4-NSUN4 protein complex that regulates

mitochondrial ribosome biogenesis. Proc Natl Acad Sci U S A 109, 15253-15258

Sprinzl M, Vassilenko KS (2005): Compilation of tRNA sequences and sequences of tRNA genes. Nucleic Acids Res 33, D139-D140

Squires JE, Patel HR, Nousch M, Sibbritt T, Humphreys DT, Parker BJ, Suter CM, Preiss T (2012): Widespread occurrence of 5-methylcytosine in human coding and non-coding RNA. Nucleic Acids Res 40, 5023-5033

Strahl BD, Allis CD (2000): The language of covalent histone modifications. Nature 403, 41-45

Suzuki MM, Bird A (2008): DNA methylation landscapes: provocative insights from epigenomics. Nat Rev Genet 9, 465-476

Suzuki T: Biosynthesis and function of tRNA wobble modifications. In: Grosjean H (ed.): Fine-tuning of RNA functions by modification and editing. Springer, Berlin, Heidelberg 2005, 23-69

Suzuki T, Suzuki T (2014): A complete landscape of post-transcriptional modifications in mammalian mitochondrial tRNAs. Nucleic Acids Res 42, 7346-7357

Suzuki T, Nagao A, Suzuki T (2011): Human mitochondrial tRNAs: biogenesis, function, structural aspects, and diseases. Annu Rev Genet 45, 299-329

Tafforeau L, Zorbas C, Langhendries JL, Mullineux ST, Stamatopoulou V, Mullier R, Wacheul L, Lafontaine DL (2013): The complexity of human ribosome biogenesis revealed by systematic nucleolar screening of pre-rRNA processing factors. Mol Cell 51, 539-551

Tahiliani M, Koh KP, Shen Y, Pastor WA, Bandukwala H, Brudno Y, Agarwal S, Lyer LM, Liu DR, Aravind L et al. (2009): Conversion of 5-methylcytosine to 5-hydroxymethylcytosine in mammalian DNA by MLL partner TET1. Science 324, 930-935

Takemoto C, Spremulli LL, Benkowski LA, Ueda T, Yokogawa T, Watanabe K (2009): Unconventional decoding of the AUA codon as methionine by mitochondrial tRNA Met with the anticodon f5CAU as revealed with a mitochondrial in vitro translation system. Nucleic Acids Res 37, 1616-1627

Tollervey D, Lehtonen H, Jansen R, Kern H, Hurt EC (1993): Temperature-sensitive mutations demonstrate roles for yeast fibrillarin in pre-rRNA processing, pre-rRNA methylation, and ribosome assembly. Cell 72, 443-457

Tuck MT (1992): The formation of internal 6-methyladenine residues in eucaryotic messenger RNA. Int J Biochem 24, 379-386

Tuorto F, Liebers R, Musch T, Schaefer M, Hofmann S, Kellner S, Frye M, Helm M, Stoecklin G, Lyko F (2012): RNA cytosine methylation by Dnmt2 and NSun2 promotes tRNA stability and protein synthesis. Nat Struct Mol Biol 19, 900-905

Tusup M, Kundig T, Pascolo S (2018): Epitranscriptomics of cancer. World J of Clin Oncol 9, 42-55

Urbonavicius J, Qian Q, Durand JM, Hagervall TG, Björk GR (2001): Improvement of reading frame maintenance is a common function for several tRNA modifications. EMBO J 20, 4863-4873

van den Born E, Vågbø CB, Songe-Møller L, Leihne V, Lien GF, Leszczynska G, Malkiewicz A, Krokan HE, Kirpekar F, Klungland A et al. (2011): ALKBH8-mediated formation of a novel diastereomeric pair of wobble nucleosides in mammalian tRNA. Nat Commun 2, 172

van Nues RW, Granneman S, Kudla G, Sloan KE, Chicken M, Tollervey D, Watkins NJ (2011): Box C/D snoRNP catalysed methylation is aided by additional pre-rRNA base-pairing. EMBO J 30, 2420-2430

Voigts-Hoffmann F, Hengesbach M, Kobitski AY, van Aerschot A, Herdewijn P, Nienhaus GU, Helm M (2007): A methyl group controls conformational equilibrium in human mitochondrial tRNA(Lys). J Am Chem Soc 129, 13382-13383

Walport LJ, Hopkinson RJ, Schofield CJ (2012): Mechanisms of human histone and nucleic acid demethylases. Curr Opin in Chem Biol 16, 525-534

Wang X, He C (2014): Dynamic RNA modifications in posttranscriptional regulation. Mol Cell 56, 5-12

Wang X, Lu Z, Gomez A, Hon GC, Yue Y, Han D, Fu Y, Parisien M, Dai Q, Jia G et al. (2014): N6-methyladenosine-dependent regulation of messenger RNA stability. Nature 505, 117-120

Wang X, Zhao BS, Roundtree IA, Lu Z, Han D, Ma H, Weng X, Chen K, Shi H, He C (2015): N(6)-methyladenosine modulates messenger RNA translation efficiency. Cell 161, 1388-1399

Watanabe Y, Tsurui H, Ueda T, Furushima R, Takamiya S, Kita K, Nishikawa K, Watanabe K (1994): Primary and higher order structures of nematode (ascaris suum) mitochondrial tRNAs lacking either the T or D stem. J Biol Chem 269, 22902-22906

Watkins NJ, Bohnsack MT (2012): The box C/D and H/ACA snoRNPs: key players in the modification, processing and the dynamic folding of ribosomal RNA. Wiley Interdiscip Rev RNA 3, 397-414

Westbye MP, Feyzi E, Aas PA, Vågbø CB, Talstad VA, Kavli B, Hagen L, Sundheim O, Akbari M, Liabakk NB et al. (2008): Human AlkB homolog 1 is a mitochondrial protein that demethylates 3-methylcytosine in DNA and RNA. J Biol Chem 283, 25046-25056

Xiao W, Adhikari S, Dahal U, Chen YS, Hao YJ, Sun BF, Sun HY, Li A, Ping XL, Lai WY et al. (2016): Nuclear m6A reader YTHDC1 regulates mRNA splicing. Mol Cell 61, 507-519

Yang X, Yang Y, Sun BF, Chen YS, Xu JW, Lai WY, Li A, Wang X, Bhattarai DP, Xiao W et al. (2017): 5-methylcytosine promotes mRNA export – NSUN2 as the methyltransferase and ALYREF as an m5C reader. Cell Res 27, 606-625

Yarham JW, Elson JL, Blakely EL, McFarland R, Taylor RW (2010): Mitochondrial tRNA mutations and disease. Wiley Interdiscip Rev RNA 1, 304-324

Yi J, Gao R, Chen Y, Yang Z, Han P, Zhang H, Dou Y, Liu W, Wang W, Du G et al. (2017): Overexpression of NSUN2 by DNA hypomethylation is associated with metastatic progression in human breast cancer. Oncotarget 8, 20751-20765

Yue Y, Liu J, He C (2015): RNA N6-methyladenosine methylation in post-transcriptional gene expression regulation. Genes Dev 29, 1343-1355

Zebarjadian Y, King T, Fournier MJ, Clarke L, Carbon J (1999): Point mutations in yeast CBF5 can abolish in vivo pseudouridylation of rRNA. Mol Cell Biol 19, 7461-7472

Zheng G, Dahl JA, Niu Y, Fedorcsak P, Huang CM, Li CJ, Vågbø CB, Shi Y, Wang WL, Song SH et al. (2013): ALKBH5 is a mammalian RNA demethylase that impacts RNA metabolism and mouse fertility. Mol Cell 49, 18-29

Acknowledgements

First and foremost, I want to thank Prof. Dr. Markus T. Bohnsack for giving me the opportunity to join his lab and Dr. Sara Haag, who worked with me on this exciting project.

Special thanks go to Dr. Katherine Bohnsack for her near endless patience, her constant support and constructive input during the whole process of writing this thesis.

I want to thank all the members of the Bohnsack group who created a unique working environment in which I have always felt comfortable and productive. The members of the “human lab”: Dr. Ahmed Warda, Dr. Indira Memet and Dr. Priyanka Choudhury as well as my colleagues from the “yeast lab”: Dr. Roman Martin, Dr. Lukas Brüning, Dr. Annika Heininger and Dr. Jimena Davila Gallesio. Philipp Hackert, who introduced me to laboratory work deserves great thanks.

Finally, I would like to express my gratitude to Dr. Carl Weidinger, Dr. Rebekka Dülk and Katharina von Knebel for reading and very carefully proofreading this thesis.

Curriculum vitae

My name is Benedikt Hübner, I was born on February 6th, 1987 in Munich, and I am currently living at Torstraße 185 in 10115 Berlin.

After attending Marsplatz Elementary School and Rudolf Steiner Schule, Schwabing, I did my Abitur in 2006 at the Michaeli Gymnasium, Munich.

Before I started studying medicine, I did a professional internship as craftsman and architect at Raw & Fine Joinery, performed community service at the Social Psychiatric Centre “Haus an der Teutoburger Straße”, worked as a waiter at Timballo Foodlounge, and as an independent journalist at Prinz Lifestyle Magazine.

Preparing for my medical degree, I worked as nursing assistant at Max Planck Institute for Psychiatry, Munich and attended a paramedic education program at Walner-Schulen, Munich. Since 2012, I have been working with international onboard stem cell transports.

From 2012 till 2019, I studied medicine at the Georg August University of Goettingen. During my studies, I worked as a lecturer for anatomy and histology, instructor, and head of our medical skills lab, and founded a weekly meditation course for medical students. Besides my work at the hospital, I worked as a paramedic at the Red Cross, Goettingen.

Inspired by basic science courses at pre-med, I started my scientific career at the Bohnsack group at the Department of Molecular Biology, University Medical Centre Goettingen. Here, I performed practical laboratory work investigating the role of the dioxygenase ABH1 in establishing a modification in a mitochondrial tRNA that is important for mitochondrial translation. The results of this work were published in the EMBO Journal and are presented in this doctoral thesis.

After finishing my studies in 2019, I moved to Berlin where I am currently a third-year resident at the Internal Medicine Department of the Red Cross Hospital, Berlin Westend. I am planning to become an internal medicine specialist before qualifying as a specialist in Psychiatry and Psychotherapy.